Geophys. J. Int. (2002) **148,** 34–57

Evolution of the Mongol–Okhotsk Ocean as constrained by new palaeomagnetic data from the Mongol–Okhotsk suture zone, Siberia

Vadim A. Kravchinsky,[1,2,3,*] Jean-Pascal Cogné[3], William P. Harbert[4], and Mikhail I. Kuzmin

[1] *East-Siberian Research Institute of Geology, Geophysics and Mineral Resources, Irkutsk* 664007, *Russia*
[2] *Institute of Geochemistry, Siberian Branch of Russian Academy of Science, Irkutsk* 664033, *Russia*
[3] *Laboratoire de Palaeomagnetisme, Institut de Physique du Globe de Paris,* 4 *place Jussieu,* 75252 *Paris Cedex* 05, *France*
[4] *Dept. of Geology and Planetary Science, University of Pittsburgh, Pittsburgh,* PA 15260, *USA*

Accepted 2001 July 6. Received 2001 May 15; in original form 2000 April 22

SUMMARY

This paper presents new data from palaeomagnetic investigations on the Upper Palaeozoic and Mesozoic geological units from the Siberian platform and the Mongol–Okhotsk suture zone. Within the southern portion of the Mongol–Okhotsk suture we collected palaeomagnetic samples from the Late Permian Belektuy formation (Borzya region; 50.7°N, 116.9°E) and the Middle–Late Jurassic Shadaron formation (Unda-Daya; 51.5°N, 117.5°E). We sampled the Late Permian Alentuy formation (Khilok region; 50.8°N, 107.2°E), the Early to Middle Jurassic Irkutsk sedimentary basin (ISB; 52.0°N, 104.0°E), the Late Jurassic Badin formation (Mogzon region; 51.8°N, 112.0°E), and the Early Cretaceous Gusinoozesk formation (Gusinoe Lake region; 51.2°N, 106.5°E) additionally in the northern region of the Mongol–Okhotsk suture.

Apart from the results of the ISB and Gusinoozersk formations, which show very large ellipses of confidence and might be the present-day geomagnetic field overprint, our results allow us to constrain the evolution of the Mongol–Okhotsk Ocean palaeomagnetically from the Late Permian to the Middle–Late Jurassic. They confirm that this large Permian ocean closed during the Jurassic, ending up in the late Jurassic or the beginning of the Cretaceous in the eastern end of the suture zone, as suspected on geological grounds. However, although geological data suggest a Middle Jurassic closure of the Mongol–Okhotsk Ocean in the west Trans-Baikal region, our data show evidence of a still large palaeolatitude difference between the Amuria and Siberia blocks. This is interpreted as a result of the quite fast closure of the ocean after the Middle Jurassic. Finally, our new palaeomagnetic results exhibit very large tectonic rotations around local vertical axes, which we interpret as probably arising both from collision processes and from a left-lateral shear movement along the suture zone, due to the eastward extrusion of Mongolia under the effect of the collision of India into Asia.

Key words: Mongol–Okhotsk Ocean, palaeomagnetism, plate tectonics, Siberia, suture.

1 INTRODUCTION

The Mongol–Okhotsk fold belt stretches over 3000 km along the southwestern boundary of the Siberia plate from the Udsky Gulf of Okhotsk Sea to Central Mongolia, through the eastern Trans-Baikal region (Fig. 1). The occurrence all along this belt of hyperbasites, ophiolites, as well as intrusions of gabbro-tonalites and plagiogranites of the Bereya and Pikan complexes, comparable with granitoids of island-arc setting, has led several authors (e.g. Zonenshain *et al*. 1976; Kuzmin & Fillipova 1979; Parfenov 1984; Zonenshain *et al*. 1990; Nei 1991; Sorokin 1992) to propose that this fold belt is a suture zone between Siberia to the north and the Amuria (or Mongolia) block to the south. Following Zonenshain *et al*. (1990), the Amuria microcontinent consists of a number of lithospheric blocks (Khangay, Khentey, Central-Mongolian, Argun, Khingan-Bureya), which accreted together in the early Palaeozoic. The felsic intrusives parallel

* Now at: Physics Department, University of Alberta, Edmonton, AB, Canada, T6G 2J1. E-mail: vkrav@phys.ualberta.ca

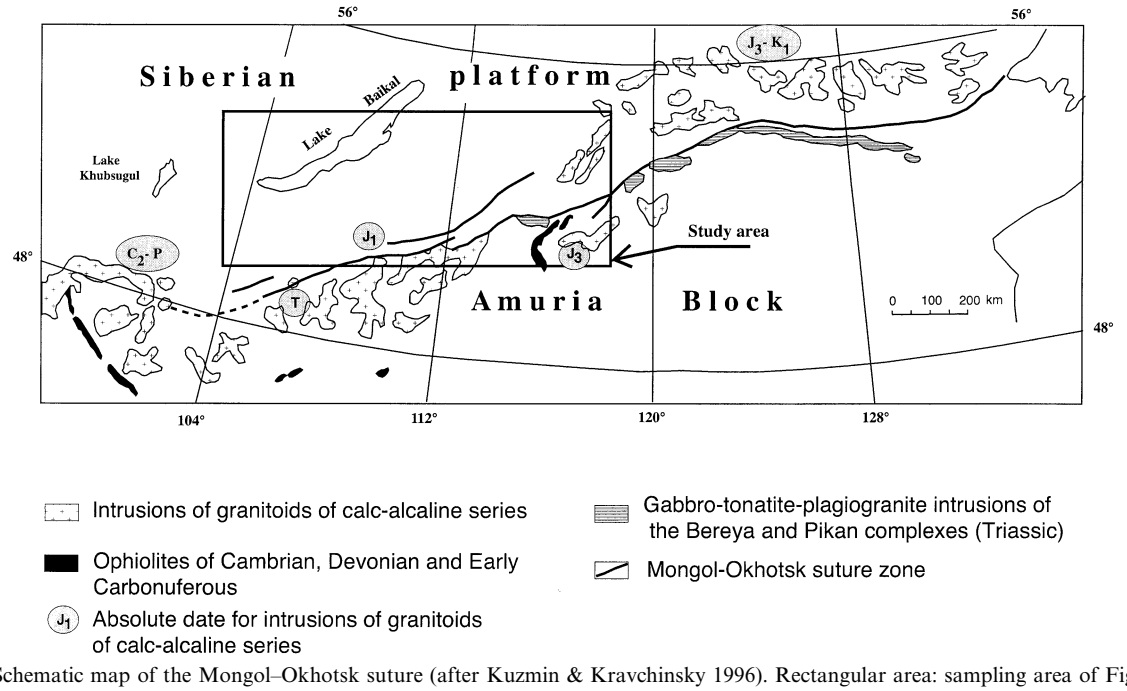

Figure 1. Schematic map of the Mongol–Okhotsk suture (after Kuzmin & Kravchinsky 1996). Rectangular area: sampling area of Fig. 2.

to the suture have been shown to young from the west to the east of the Mongol–Okhotsk suture zone (Fig. 1), going from Late Carboniferous–Permian in Central Mongolia, to Triassic–Early Jurassic in west Transbaikalia, Late Jurassic in east Transbaikalia, and Cretaceous in the Amur province, the far-eastern part of south Siberia (Kuzmin 1985; Zonenshain & Kuzmin 1997). This has been interpreted as resulting from a progressive, long-lasting history of collision between Amuria and Siberia, beginning at the end of the Carboniferous in the west, and finishing in the east at the beginning of the Cretaceous.

From a palaeomagnetic point of view, Xu *et al.* (1997) found evidence of a large palaeolatitude discrepancy between Amuria and Siberia in the Permian. Their data, which come from the Chita region, south of the suture, will be re-appraised in the present paper, including our new data from the region evaluated. A preliminary palaeomagnetic study of Cretaceous effusives from the Amur province (Halim *et al.* 1998a) appears to confirm that the Mongol–Okhotsk Ocean was closed by the Early Cretaceous. Farther to the south, geological and palaeomagnetic evidence (Pruner 1992) shows that Amuria and the North China Block were accreted earlier, by the Late Carboniferous. Palaeomagnetic data from the North and South China Blocks (NCB and SCB, Enkin *et al.* 1992; Gilder & Courtillot 1997; Yang & Besse 2001) are consistent with this model. The data show that the continental landmass composed of Amuria, the NCB and the SCB was not accreted to Siberia before the Cretaceous, implying the existence of a large oceanic space, the Mongol–Okhotsk Ocean, between Amuria and Siberia before that time.

Finally, apart from first results of Kravchinsky (1990, 1995) and Kuzmin & Kravchinsky (1996), which were published in Russian, no detailed palaeomagnetic results are available from within the suture zone itself. In order to remedy this situation, we present here new and more complete results of the palaeomagnetic analysis of samples from five localities situated on both sides of the Mongol–Okhotsk suture zone, with ages ranging from the Late Permian to the Early Cretaceous.

2 GEOLOGICAL SETTING

In order to constrain the evolution and the time of closure of the Mongol–Okhotsk Ocean better, we sampled six localities of palaeontologically dated Late Permian to Early Cretaceous sedimentary formations from both the northern and southern sides of the Mongol–Okhotsk suture (Fig. 2). Except for locality 4, which is situated on the southern edge of the Siberian platform, these localities were sampled within the Trans-Baikal area, which separates this platform from Inner Mongolia and the NCB.

2.1 South of the Mongol–Okhotsk suture zone

2.1.1 The Late Permian Belektuy formation of the Borzja region

The Late Permian Belektuy formation of the Borzja region (Chita province, locality 1 in Fig. 2; 50.65°N, 116.88°E) is part of the largest Permian exposure within the East Trans-Baikal area (Nalivkin 1966). Stratigraphically, this formation begins with a unit of sandy-clay deposits grading into various pebble conglomerates (about 400 m thick), followed by three members of interbedded sandstones, siltstones, tuffites and tuffs, with occasional silica beds at the bottom, for a total thickness of 900–1300 m. The faunal remains from the middle part of the section are represented by the Kazan complex species, namely *Athyris* (*Cleithyridina*) *pectinifera Sow.*, *Aviculopecten ax gr sublatratus Keys.*, *Liebea septifera King.*, *Z. cf. hausmanni Goldf.*, *Schizodus subobcurus Lich.*, *Sch. netcshajewi Zich.* (Nalivkin 1966). Structurally, the Borzya region consists of a large syncline about 80 km long, with a syncline width of up to 25 km. Regionally, this simple geometry is occasionally complicated by second-order folding within the central region of the structural belt. The western limb of the syncline is partly overlapped by Jurassic and younger formations, while the eastern wing is truncated by a regional zone of faults.

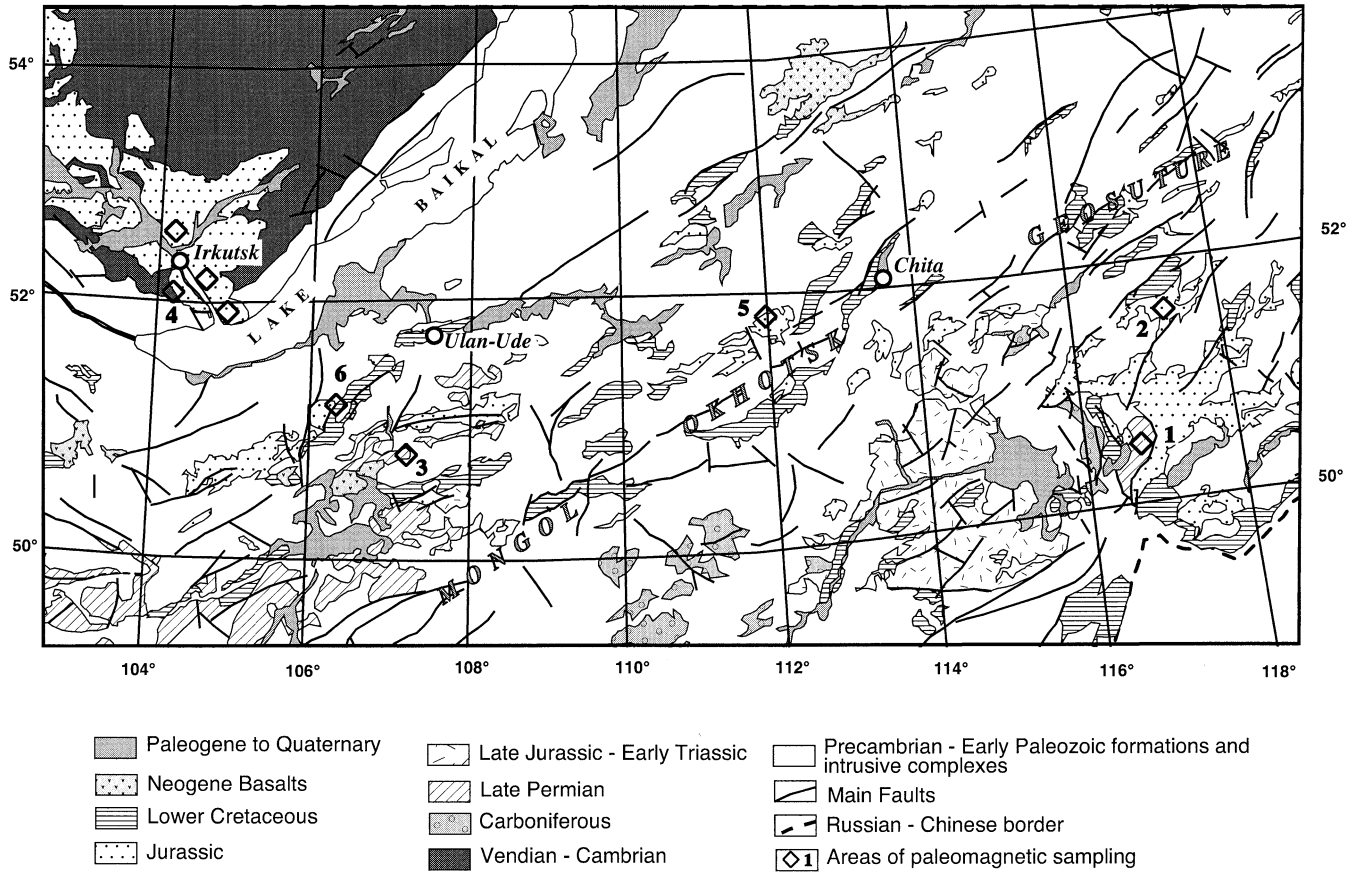

Figure 2. Simplified geological map of the southern border of the Siberian platform and western Trans-Baikal region (after Yanshin (1981) with palaeomagnetic sampling localities of the present study (diamonds). The localities are 1: Borzja region (Belektuy formation, Late Permian); 2: Unda-Daya Depression (Shadaron formation, Middle–Late Jurassic); 3: Khilok river region (Alentuy formation, Late Permian); 4: Siberian platform, (Early–Middle Jurassic sediments, Irkutsk sedimentary basin); 5: Mogzon region (Badin formation, Late Jurassic); 6: Gusinoe Ozero Depression (Gusinoozersk serie, Early Cretaceous).

56 oriented blocks of the Belektuy formation were sampled at 11 sites from a 250 m wide outcrop along the left bank of the Belektuy River, 4 km upstream of Belektuy village. The rocks occur monoclinally at this place, with some small deviation. The azimuth of dip is from 175° to 235°, and the dip from 36° to 57°. An orientation of each sampled block was measured in the field independently, and was used for further calculations.

This sampling completes a first study of 26 sites (5–10 oriented cores from each site) from this formation made by Xu *et al.* (1997).

2.1.2 Middle–Late Jurassic Shadaron and Tergen formations of the Unda-Daya Depression

The locality of the Shadaron formation (Middle–Late Jurassic) was sampled along the right bank of the Unda River near the village of Tergen in Chita province (locality 2 in Fig. 2; 51.5N°, 117.5°E). The Shadaron formation consists of interbedded conglomerates and sandstones with rare siltstone beds (Sinitsa & Starukhina 1986). Conglomerate beds, 100–120 m thick, are found in the lower and upper parts of the formation. A horizon of basalts, andesites, lava breccias, and tuff breccias is recognized at the base of the section. The age of this formation is based on the occurrence of insects, bivalves, conchostracans, ostracods, notostraca, and horsetails (Skoblo & Lyamina 1985; Sinitsa & Starukhina 1986). Typical Middle–Late Jurassic forms were determined, as well as mollusks and palaeoplants from the Late Jurassic. Absolute age determination (K–Ar method) in the lowest part of the formation gives a result of around 163–167 Ma (Shubkin *et al.* 1992). Thus the geological age of the formation was accepted as Middle–Late Jurassic (Shubkin *et al.* 1992).

We sampled 80 oriented blocks from 15 sites from a generally monoclinal structure (with some deviations) along the right bank of the Unda River (possibly only the Upper Jurassic part of the Shadaron formation). These were taken from volcanic (basalts, andesites) and volcanogenic-sedimentary (tuffs, sandstones) lithologies of the formation. The orientation of interbedded volcanic rocks was recorded after measuring elements of the bedding orientation in sediments: azimuth of dip between 300° and 35°; dip between 10° and 30°. Sampling was made in stratigraphic order from lower (site 1-1) to upper parts of the formation (site 2-2).

2.2 North of the Mongol–Okhotsk suture zone

2.2.1 The Late Permian Alentuy formation of Khilok region

The deposits of the Alentuy formation of Late Permian age (Sizykh & Shaposhnikov 1971) were sampled within the

Khilok River basin along the Alentuy River (locality 3 in Fig. 2; 50.8°N, 107.2°E). The 400–2000 m thick formation consists of subalkaline extrusive units and tuffs interbedded with beds of sandstones, conglomerates, and siltstones. This complex is intruded by granitoids, and both are overlapped by Jurassic deposits and thrusted over the underlying units. The age of the Alentuy formation is constrained by a Late Permian flora (Kozubova & Radtchenko 1961): *Grassinervia cf. pentagonata Gorel*., *Cordaites cf. mitinaensis* (*Goreb.*), *S. Meyen*., *Compsopteris sp. Paracalamites sp*., *Noeggerathiopsis cf. anomala Radcs*., *Calyccarpus crassus*. The 92 oriented blocks (3–4 oriented samples from each block) from 15 sites were taken throughout the section of the left bank of Alentuy River, 2 km upstream from river-mouth to Khilok River. We sampled various lithologies of rocks, such as lavas, tuffs of andesitodacites, intrabedded sandstones and siltstones. We used the tilt orientation of interbedded sediments for stratigraphic corrections of lava flows (listed in Table 3). The age of folding in the region is poorly constrained and may range from the Cretaceous to the Cenozoic (Likhanov 1991).

2.2.2 *The Irkutsk Jurassic basin of the Siberian platform*

Lower–Middle Jurassic rocks from south of the Siberian platform were sampled around the city of Irkutsk, in the so-called Irkutsk Basin (locality 4, Fig. 2; average location: 52.0°N, 104.0°E). The Irkutsk Basin was deposited during the Jurassic in response to a large pulse of sedimentary material (sandstones, fine sandstones and gravels) coming from the Trans-Baikal region. The sedimentary facies suggest that well-developed river systems, lakes and swamps existed during a warm climatic period in Siberia (Neustroeva 1988). Then, a slow uplift took place in the central Siberian region during the Aalenian. The Lena Sea, which had covered some northern parts of the Siberian platform, regressed and coal deposits gradually stopped, but continental lakes with mainly clay facies sediments remained (Skoblo *et al*. 1994).

Recent detailed stratigraphic and palaeontological studies of pollens, flora and fauna (Skoblo & Lyamina 1985; Skoblo *et al*. 1991, 1994; Lyamina *et al*. 1998) provide excellent estimates of the age of the various Jurassic units composing this basin. These units are composed of yellow and brownish sandstones and pelites with various grain sizes and numerous coal horizons. Oriented cores were taken at 16 sites distributed around Irkutsk: three sites (J14–16, Table 4) in the Pliensbachian (J_1) Cheremkhovo formation, six sites (J1–6) in the Pliensbachian–Toarcian (J_1) Ust-Baley formation, two sites (J7–8) in the Pliensbachian to Aalenian (J_1/J_2) Taltsinka formation, and five sites (J9–13) in the Aalenian (J_2) Sukhovskoy formation (e.g. Lyamina *et al*. 1998). The regional attitude of all these sedimentary beds is subhorizontal, with bedding dips varying between 0° and 12° at different sites.

2.2.3 *The Late Jurassic Badin formation of Mogzon region (Chita province)*

The Late Jurassic Badin formation of Mogzon region is widespread in the Khilok-Uda basin in Chita province (locality 5, Fig. 2; 51.8°N, 112.0°E). The rocks of the Badin formation make up the Mogzon Trough, a typical volcano-dome structure, formed as a result of multiple eruptions of central-type volcanoes. As a result, a complex of volcanogenic and volcano-sedimentary formations accumulated in a series of smaller volcano-tectonic structures (Likhanov 1991). Palaeontological and stratigraphic studies of the reference sections of the sedimentary–tuffaceous unit (Skoblo & Lyamina 1985) provided Late Jurassic fossil insects: *Chironomaptera Scobloi Kalug*., *Orychochlus longilobus Kalug*., *Tophocladius stygalis lyg*., *Orychlus longilobus Kalug*., *Tophocladius stygialis lug*., *Orychochlus longilobus Kalug*., *Tophocladius stygialis Kalug*., *Mogsonurus ceraius Vishn*., *Zopapsocus cf. parvulus Vishn*; and flora: *Tallites sp*., *Eguisetites sp*., *Cladophlebis sp*., *Brachyphyllum sp*., *Schizolepis sp*. The formation is 900–1150 m thick.

57 oriented blocks (3–4 samples from each block) were sampled at 14 sites from five bulldozed trenches at the top of the middle subformation, 50 km north of Mogzon village. The section is represented by interbedded white, green-white, and yellow-white tuffs and tuffaceous sandstones. There are considerable variations in strikes and dips of the strata: the azimuth of dip is 270° to 330°, and the dip 7° to 33°. The last outcrop (sites 9-1 to 9-3) is not dated by palaeontology, and is separated from the other sites by faults and rhyolite intrusions. These geological data suggest that these two groups may have different ages (Likhanov 1991).

2.2.4 *Early Cretaceous formations of Gusinoe lake*

Early Cretaceous rocks are widespread in the south of the Buryat Republic. We investigated sedimentary rocks in the Gusinoe lake region (Gusionoozersk Depression, locality 6 in Fig. 2; region around 51.2°N, 106.48°E). At this place, the units, which are made of repeated two-member transgressive rhythms of sediments (from gravelstones to siltstones) with intercalated beds of highly mature brown coal, have been dated as Early Cretaceous from the occurrence of ostracods (Skoblo & Lyamina 1982) and dinosaurs, turtles and fish remains (Dmitriev & Rozhdestvensky 1968). Oriented cores were collected at 12 sites from three Early Cretaceous members of the sequence, on the northwestern and southeastern shores of Gusinoe lake: six sites (K23–K28) in the Murtoy formation of Berriasian–Valanginian age (Skoblo & Lyamina 1982), on the northwestern shore of the lake; four sites (K17, K18, K21, K22) in the upper part of the Selenga formation of Hauterivian–Barremian age; and two sites (K19, K20) in the Khalbodzhin formation of Barremian–Aptian age, on the southeastern termination of the lake. The bedding orientation is subhorizontal with some deviation (from 5° to 20°).

Tectonic processes played an important role in the formation of the Gusinoozersk depression. The lake, with fossils of dinosaurs, originated at the beginning of the Early Cretaceous (Skoblo & Lyamina 1982) and was the final runoff water reservoir from the Pre-Khambinsky Ridge. Later, judging from geological and palaeontological data, the lake expanded and deepened, having occupied the entire depression or its larger part. It is most probable that such a transformation of the landscape for tectonic reasons proceeded very fast rather than by continuous evolution. Higher in the cross-section of the Gusinoozersk series (southeastern termination of the lake) the coal-bearing sequence shows two phases of rejuvenated movements through the Monostoy fault, which resulted in the relief changes.

3 PALAEOMAGNETIC METHODS

The samples were subjected to stepwise thermal and AF demagnetizations in the palaeomagnetic laboratories of the East-Siberian Research Institute and Institute of Geochemistry (Irkutsk, Russia), the Institut de Physique du Globe de Paris (France), and the University of Pittsburgh (USA).

In Irkutsk, the samples of all the formations presented in the paper were heated and cooled in a non-magnetic oven placed within a triple μ-metallic shield (development by V. P. Aparin, Institute of Physics, Krasnoyarsk). In the centre of the oven, the residual field is about 8 nT. Measurements of the remanent magnetization were made with a JR-4 spinner magnetometer. Magnetic susceptibility was measured with a KLY-2 Kappa-bridge (Jelinek 1966, 1973).

The magnetization of the Irkutsk Jurassic basin and Early Cretaceous rocks was measured with a cryogenic magnetometer (CTF Superconducting Rock Magnetometer, SRM) in the palaeomagnetic laboratory of the Institut de Physique du Globe de Paris. For purposes of inter-laboratory comparison, 10 per cent of these samples were demagnetized in the palaeomagnetic laboratory of Irkutsk. About 20 per cent of all the other samples were demagnetized in the Paris laboratory. The results of the two laboratories have a very high level of coincidence. Demagnetization by alternating magnetic fields (AF) of various amplitudes turned out to be ineffective for these sediments, and the majority of samples were therefore thermally demagnetized. Changes of magnetic mineralogy during thermal demagnetization were monitored by measurements of magnetic susceptibility after each heating step.

Some samples from the Late Permian Belektuy formation (from three sites, Sib39, 47 and 51, out of a possible 14; Table 1) were measured with a three-component 2G SRM and thermally demagnetized using a large-capacity ASC model TD-48 oven, installed in the magnetically shielded room at the University of Pittsburgh (the total field in the cooling region of the oven is about 5 nT). The results were published by Xu *et al.* (1997). The remaining 11 sites (Sites b1 to b11; Table 1) were studied in Irkutsk. All measuring results coincide between the two laboratories, and in the following the results from the two studies will be discussed together.

Changes in the intensity and direction of remanent magnetization vectors during demagnetization experiments were analysed using orthogonal vector end-point projections (Zijderveld 1967). The magnetic component directions were identified using principal component analysis (PCA) (Kirschvink 1980), or remagnetization great-circle methods (Halls 1976). Site-mean directions were determined using Fisher (1953) statistics or, in the case of combined directional data and remagnetization circles (always with sector constraints method), McFadden & McElhinny (1988) statistics.

The data were processed using the palaeomagnetic data treatment OPAL system, created for an IBM-PC computer in the Irkutsk laboratory (Vinarsky *et al.* 1987), the PalaeoMac application developed at the Institut de Physique du Globe de Paris (IPGP) by J. P. Cogné, and a package of programs developed by R. Enkin (Enkin 1990, 1996).

Table 1. Site-mean palaeomagnetic directions for the high-temperature component for Belektuy formation rocks (Late Permian; locality coordinates: 50.65°N, 116.88°E)

Site	*n*	D_g	I_g	D_s	I_s	*k*	α_{95}	N/R	Notes
b1	9	294.2	−10.5	305.6	−21.8	8.5	19.3	R	(4d + 5cc)
b2	5	53.3	0.3	63.9	33.5	12.2	23.4	N	4d + 1cc
b3	6	286.1	−49.1	–	–	8.2	24.8	R	6d
		–	–	319.9	−23.0	9.6	22.7		
b4	8	244.9	−27.3	–	–	5.2	27.6	R	3d + 5cc
		–	–	287.1	−45.1	5.5	26.9		
b5	8	220.0	33.8	–	–	5.4	27.0	R	3d + 5cc
		–	–	267.1	−39.6	6.1	25.4		
b6	6	83.1	45.5	116.5	41.3	19.2	15.9	N	5d + 1cc
b7	9	214.1	−66.5	–	–	4.1	29.0	R	4d + 5cc
		–	–	313.2	−43.0	4.8	26.7		4d + 5cc
b8	5	103.2	31.3	126.4	32.0	41.1	12.9	N	3d + 2cc
b9	8	229.1	−26.9	–	–	25.6	12.1	R	2d + 6cc
		–	–	257.0	−58.2	10.5	19.2		
b10	9	268.5	−42.4	–	–	7.8	20.3	R	4d + 5cc
		–	–	306.4	−35.0	10.4	17.3		
b11	5	270.2	−23.9	–	–	8.7	28.2	R	4d + 1cc
		–	–	291.4	−18.8	7.6	30.4		
Sib39 *	3	246.2	−47.0	249.6	−47.0	27.8	23.8	R	
Sib47 *	4	44.5	13.0	46.1	22.4	16.6	23.2	N	
Sib51 *	5	86.9	−3.7	90.1	14.4	53.9	10.5	N	
	14	74.1	30.2	–	–	6.8	16.4		
	sites	–	–	102.8	37.4	9.2	13.8		

n: number of directions and great circles accepted for calculation; *D* (*I*): declination (inclination) of the characteristic component of NRM in a geographical (g) or stratigraphic (s) system of coordinates; *k*, α_{95}: precision parameter and half-angle radius of the 95 per cent probability confidence cone; N/R: number of directions of the normal/reversal polarity. d or cc in Notes gives the number of directions or great circles accepted for calculations. * denotes accepted mean directions from Xu *et al.* (1997) with $\alpha_{95} < 30°$.

4 PALAEOMAGNETIC RESULTS

4.1 South of the Mongol–Okhotsk suture zone

4.1.1 The Late Permian Belektuy formation of the Borzja region

As stated above, 26 sites have already been analysed and discussed by Xu *et al.* (1997). For the 11 sites of the present study, the fine- to medium-grained sandstones of the Late Permian Belektuy formation exhibit low values of natural remanent magnetization (NRM), magnetic susceptibility (χ), and Koenigsberger ratio (Q). NRM averages 0.45 mA m^{-1}, $\chi = 10.56 \times 10^{-6}$ SI units, and $Q = 0.15$. NRM directions cluster around the present-day direction of the geomagnetic field in the region ($D = 351.5°$, $I = 68.8°$).

Thermal demagnetization of the samples (Fig. 3) enabled us to isolate two magnetization components. A low-temperature

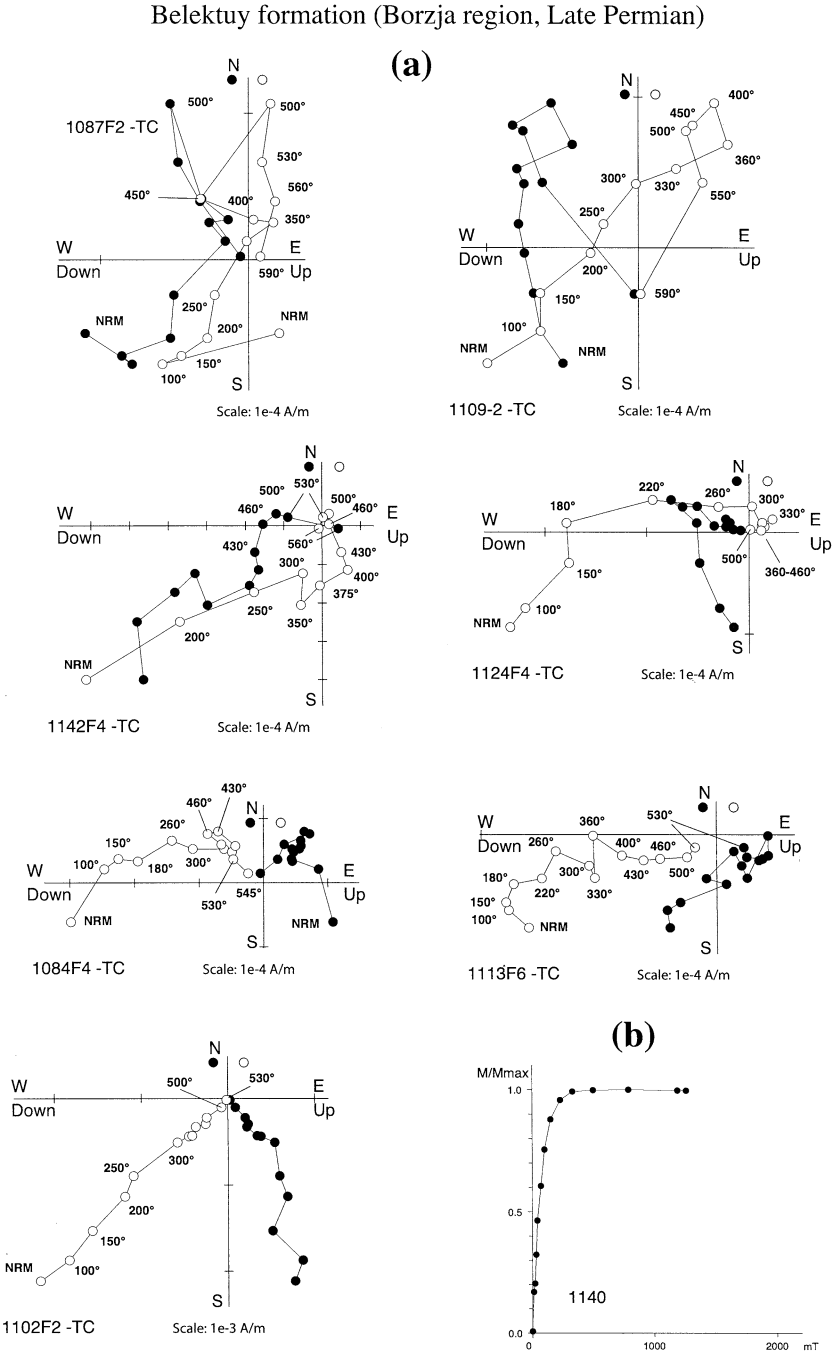

Figure 3. Results of rock-magnetic and thermal demagnetization experiments for Belektuy formation (Borzja region, Late Permian) sediments. (a) Typical orthogonal vector plots (Zijderveld 1967), in tilt-corrected coordinates; closed (open) symbols: projection onto the horizontal (vertical) plane. Temperatures are indicated in °C. (b) Isothermal remanent magnetization (IRM) acquisition in fields of up to 1.2 T showing the presence of a low-coercivity magnetic mineral.

component (LTC) is removed after heating up to 250–300 °C and makes up about 90 per cent of the total NRM intensity. This component coincides with the present-day geomagnetic field in geographical (i.e. before tilt-correction) coordinates. At the site level, the Fisher (1953) average of this component in geographical coordinates is $D_g = 355.9°$, $I_g = 72.3°$; $k_g = 37.1$, $\alpha_{95} = 7.6°$, $n = 11$ sites, and in stratigraphic coordinates it is $D_s = 195.3°$, $I_s = 64.1°$; $k_s = 26.9$, $\alpha_{95} = 9.0°$. Application of the fold test (McElhinny 1964) for the LTC gives a maximum at 35.5 per cent, $k_g/k_s = 1.38$ (fold test inconclusive). The fold test of Watson & Enkin (1993) gives a similar result (35.5 per cent of maximum unfolding). However, because of its direction, and of the low unblocking temperature of this component, we interpret it as a recent overprint, probably of weathering origin.

After this LTC, the high temperature component (HTC) unblocks between 450 and 590 °C (Fig. 3). This temperature range, together with the low-coercivity minerals evidenced by the isothermal remanent magnetization (IRM) acquisition curves (Fig. 3b), shows that magnetite is the most likely carrier of this component. This HTC could be isolated in only 50 per cent of the samples. About 50 per cent of the rest of the samples displayed remagnetization great circles, and the McFadden & McElhinny (1988) statistics were used to determine the site-mean directions of the HTC.

Owing to the very low intensity of the HTC, the site-mean directions as well as the formation mean direction are quite scattered, as evidenced by the generally low values of the Fisher (1953) k parameters of the averages (Table 1). Because of this we have included in Table 1 sites with $\alpha_{95} < 30°$ instead of the usual $< 15°$–$20°$. From the 26 sites studied by Xu *et al.* (1997), we have chosen only three with the number of samples > 3 and α_{95} less then 30°. All other sites of Xu *et al.* (1997) have either $\alpha_{95} > 40°$ or the number of samples < 3. The whole population of the HTC, including the three sites of Xu *et al.* (1997) and the 11 sites from the present study, which are listed in Table 1 in stratigraphic order (e.g. site b1 at the bottom, and site b11 at the top of the sequence), shows either normal or reverse palaeomagnetic directions at the site level (Table 1, Fig. 4a), and tends to cluster upon unfolding. Although both polarities have been obtained, the reversal test (McFadden & Lowes 1981; McFadden & McElhinny 1990) performed in tilt-corrected coordinates is indeterminate (classification 'I' of McFadden and McElhinny), due to the large critical γ-value of 28.3° obtained for this population. Because of the monoclinal dipping of beds, the conventional fold test (McElhinny 1964) is inconclusive at the 95 per cent probability level. However, the Watson & Enkin (1993) fold test, based on 1000 trials, gives an optimum data grouping at 103.1 per cent of unfolding, with 95 per cent confidence limits at 75.3 and 129.0 per cent. That estimate is very near 100 per cent of untilting, and indicates that remanence is probably pre-tilting. Similarly, the fold test of Enkin (1990) gives a positive result (DC slope $= 1.105 \pm 0.692$). It is known that the age of folding in the region might be linked to the closure of the Mongol–Okhotsk Ocean (Zonenshain *et al.* 1990) and/or to the post-collisional shortening and rotations of blocks due to the penetration of India into Eurasia (Halim *et al.* 1998a). It may therefore span from the Jurassic to the Cenozoic. Taking all the evidence together, but without very strong arguments, we therefore assume that the average direction of the HTC is the primary Late Permian magnetization of this formation. The average tilt-corrected direction is $D_s = 102.8°$, $I_s = 37.4°$; $k_s = 9.2$, $\alpha_{95} = 13.8°$, $n = 14$ sites.

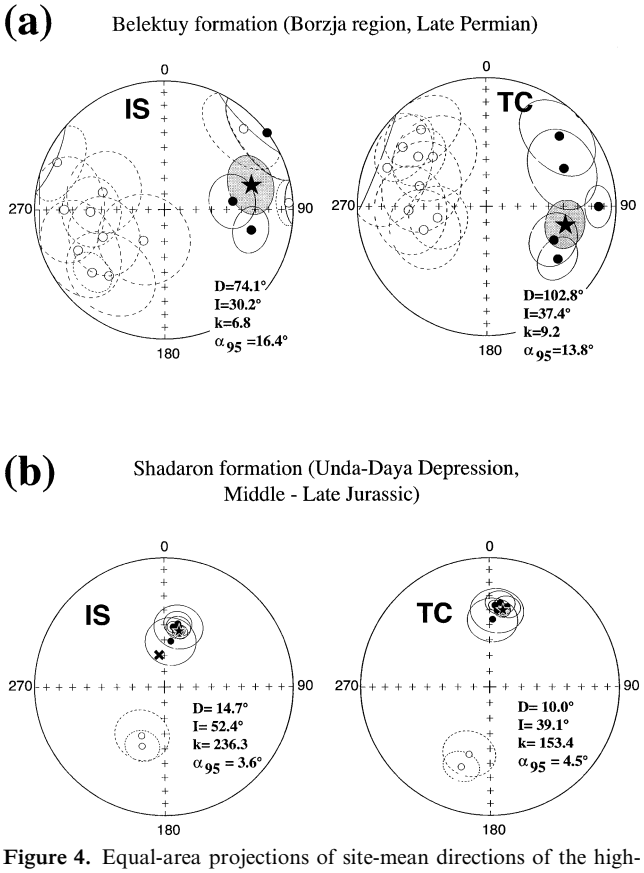

Figure 4. Equal-area projections of site-mean directions of the high-temperature component (HTC) with their α_{95} circles of confidence shown in *in situ* (left) and tilt-corrected (right) coordinates, for (a) Belektuy formation (Late Permian, Borzja region) and (b) Shadaron formation (Middle–Late Jurassic, Unda-Daya Depression). Closed (open) symbols: downward (upward) inclinations. Star: formation mean directions. Cross: present-day magnetic field direction.

4.1.2 The Middle–Late Jurassic Shadaron formation of the Unda-Daya Depression

The different lithologies for example andesites and andesite-basalts, and sediments (sandstones, tuff-sandstones) sampled in the Unda-Daya depression have two different values of initial magnetic parameters. The first group of andesite and andesite-basalt samples shows typical values for igneous rocks, with high values of NRM intensity (0.5 A m^{-1}), magnetic susceptibility ($\chi \cong 300 \times 10^{-6}$ SI units) and Koenigsberger ratio Q (2.7). The second group of sediments has relatively lower values of these parameters: NRM $\cong$ 4.5 mA m^{-1}, $\chi \cong 10 \times 10^{-6}$ SI units, $Q = 0.7$.

As demagnetization diagrams for sediments showed the LTC, or great circles for the HTC in some cases, we discuss only the volcanic rock study below. The thermal demagnetization of the Shadaron (Middle–Late Jurassic, Fig. 5) volcanic samples isolates two, sometimes three, magnetic components. The LTC is demagnetized by 400–500 °C, and its average direction at the sample level is $D_g = 353.8°$, $I_g = 78.4°$; $k_g = 44.8$, $\alpha_{95} = 3.3°$, $n = 43$ samples, in geographical coordinates. It is very close to the present geomagnetic field in the sampling region ($D = 351.1°$, $I = 69.4°$), and we therefore assume that it is a present-day overprint. The HTC demagnetizes between 500 and 590 °C, and it appears to be better resolved in normal than in reverse polarity (Fig. 5a). In some cases, when the demagnetization path does

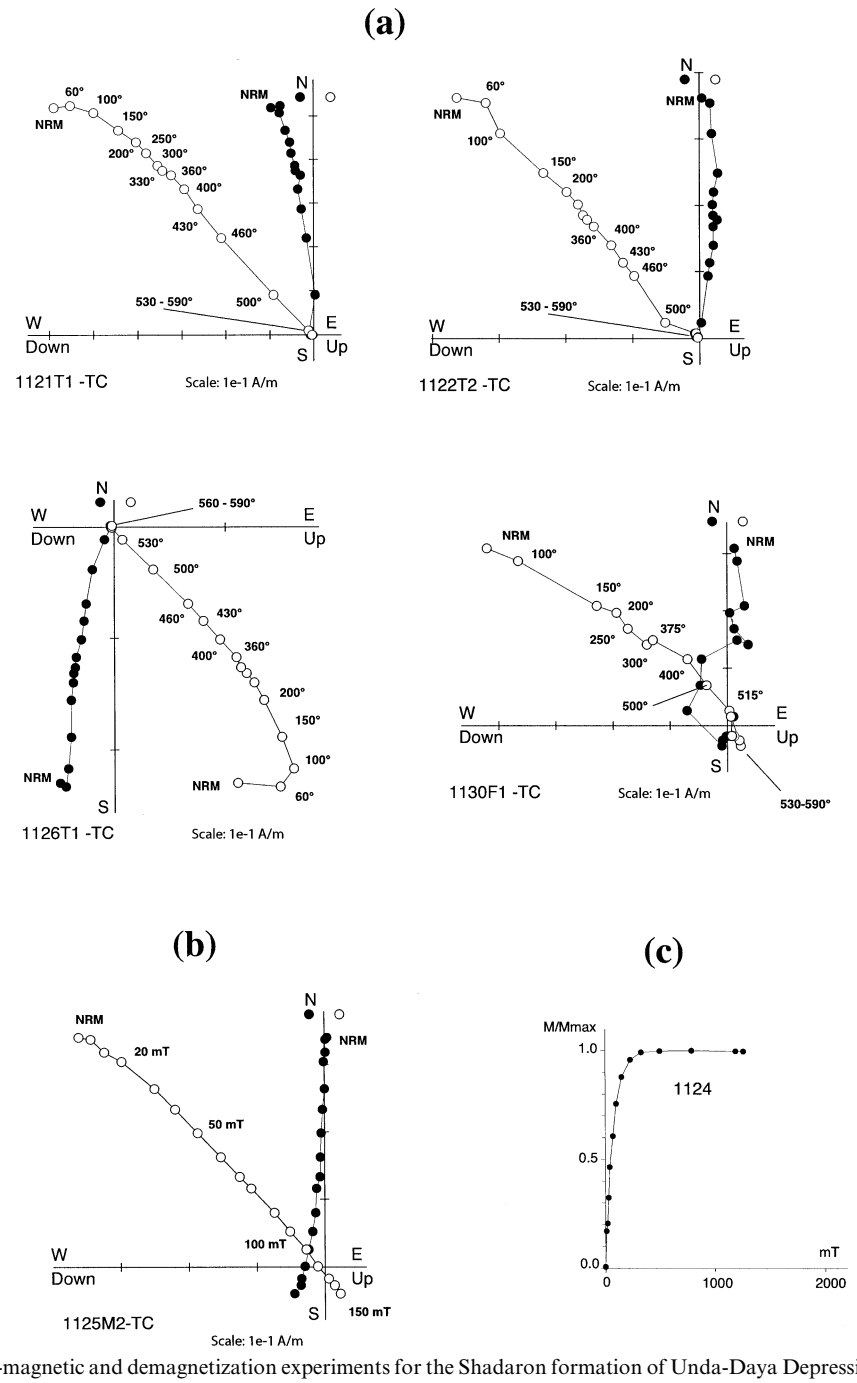

Figure 5. Results of rock-magnetic and demagnetization experiments for the Shadaron formation of Unda-Daya Depression (Middle–Late Jurassic). (a) Typical orthogonal vector plots (Zijderveld 1967), in tilt-corrected coordinates, for thermal demagnetizations (steps indicated in °C). (b) Alternating field (AF) demagnetization (steps indicated in mT). Symbols: same conventions as in Fig. 3. **(c)** IRM acquisition in fields of up to 1.2 T showing the presence of a low-coercivity magnetic mineral, possibly magnetite.

not converge towards the origin, the great-circle method was used. Some AF demagnetization experiments were performed (Fig. 5b), but they did not enable us to resolve this component clearly. The majority of AF demagnetizations are not directed towards the origin in the diagrams. On the basis of IRM experiments (Fig. 5c), which display low-coercivity minerals and thermal unblocking temperatures (500–590 °C), we conclude that magnetite might be the carrier of the HTC for this formation.

Although the between-site k parameter tends to decrease on unfolding, and probably because of small deviations among the beds, the fold test (McElhinny 1964) is inconclusive in the formation (Table 2, Fig. 4b). The fold test simulation using Watson & Enkin's (1993) method does not determine a maximum degree of untilting. This means that the fold test is ambiguous, and thus also inconclusive. All sites of Table 2 are listed in stratigraphic order, from the bottom to the top of the

Table 2. Site-mean palaeomagnetic directions for the high-temperature components for Shadaron formation rocks (Middle–Late Jurassic; location: 51.5°N, 117.5°E).

Site	*n*	D_g	I_g	D_s	I_s	*k*	α_{95}	N/R	Notes
1-1	4	8.2	60.5	–	–	35.9	15.5	N	4d
		–	2.7	46.4	9.8	14.8			
1-2	5	200.6	−49.1	199.8	−34.1	85.7	10.4	R	1d+4cc
1-3	4	13.4	50.7	–	–	153.9	7.4	N	4d
		–	12.6	36.4	149.0	7.6			
1-4	4	16.2	53.3	9.5	39.7	402.1	4.6	N	4d
1-5	6	12.3	48.4	7.4	34.4	64.3	8.4	N	6d
1-6	7	8.5	51.0	4.0	36.7	275.9	3.6	N	7d
2-1	5	204.9	−55.5	–	–	33.6	16.6	R	1d+4cc
		–	197.2	−44.1	38.5	15.5			
2-2	6	13.5	50.1	–	–	22.0	14.6	N	6d
		–	5.8	39.8	20.1	15.3			
	8	14.7	52.4	–	–	236.3	3.6		
	sites	–	–	10.0	39.1	153.4	4.5		

Same abbreviations as in Table 1.

sampling locality; that is, site 1-1 has the lowest stratigraphic position in the sampled section and site 2-2 the highest. Two palaeomagnetic polarities have been recovered, with six sites with normal polarity and two sites with reverse. However, the reversal test (McFadden & McElhinny 1990) is only marginally significant, with a critical $\gamma = 8.9°$, and the angle between the two populations (reverse and normal) being 9°. We may, however, question the significance of this test with only two reverse data. Only new studies will solve this problem.

With the lack of any positive fold or reversal test it is difficult to access the primary origin of this magnetization. We note, however, (1) the presence of both polarities, and (2) the fact that the *in situ* mean direction ($D_g = 14.7°$, $I_g = 52.4°$; $\alpha_{95} = 3.6°$; Table 2) matches neither the present-day geomagnetic field direction (Fig. 5) nor any palaeomagnetic field direction deduced from the Eurasia APWP (Besse & Courtillot 1991) or North China Block (Zhao *et al.* 1996; Enkin *et al.* 1992; Gilder & Courtillot 1997) for geological times younger than the Jurassic. We therefore make the assumption that the HTC is the primary palaeomagnetic direction of the Shadaron formation (the formation mean direction in stratigraphic coordinates $D_s = 10°$, $I_s = 39.1°$; $\alpha_{95} = 4.5$). The *in situ* HTC direction is close to the Late Jurassic NCB and Inner Mongolian area directions (south of the Amuria block; Zhao *et al.* 1990). There is no strong geological evidence that all magmatism took place at the same time as the sedimentation forming. We cannot exclude that some magmatic events occurred after sediment forming and titling. In this case in-situ coordinates pole might be more probable.

4.2 North of the Mongol–Okhotsk suture zone

4.2.1 The Late Permian Alentuy formation of Khilok region

Two types of lithologies from the Alentuy formation were sampled, andesite and dacite on the one hand, and sandstone on the other. Andesite and dacite have average magnetic values of NRM = 3 mA m^{-1}, magnetic susceptibility $\chi = 3.6 \times 10^{-6}$ SI units and $Q = 1.4$. Sandstones have slightly higher values, probably because of alteration: NRM = 6.1 mA m^{-1}, $\chi = 8.5 \times 10^{-6}$ SI units, $Q = 1.2$.

During thermal demagnetization of both rock types of the Alentuy formation (Figs 6a to e), two magnetization components were resolved. First, a LTC demagnetizes between room temperature and 300–430 °C. On the sample level, this LTC averages at $D_g = 4.0°$, $Ig = 69.6°$; $k_g = 14.9$, $\alpha_{95} = 7.7°$ in geographical coordinates. The fold test (McElhinny 1964) is negative at the 99 per cent confidence level, with the ratio of precision parameters $k_g/k_s = 3.4$ for $n = 25$. Moreover, the *in situ* direction conforms to the present-day geomagnetic field in the region ($D = 355.3°$, $I = 70.1°$). We therefore interpret the LTC as a post-folding recent magnetization overprint.

The HTC trends towards the origin of the orthogonal projections (Fig. 6), with an unblocking temperature range of 400–500 °C to 560–610 °C with generally steep negative inclinations in tilt-corrected coordinates (Figs 6a to d). IRM experiments (Fig. 6f), which evidence low-coercivity magnetic minerals, together with the observed thermal unblocking range, suggest that magnetite is the carrier of the HTC. There is no difference between the directions of the HTC for sandstones, tuffs and andesites-dacites in terms of secular variations of the geomagnetic field, as evidenced by the within-site grouping parameters (Table 3, Fig. 7a).

The site-mean directions cluster upon unfolding, with an increase of *k* parameter from 6.8 *in situ* to 23.4 after tilt-correction. The ratio of precision parameters ($k_s/k_g = 3.45$) is higher than the critical value at the 99 per cent confidence level (2.47), and the fold test (McElhinny 1964) is therefore positive. The fold test of Watson & Enkin (1993), based on 1000 trials, gives an optimum data grouping at 105.9 per cent of unfolding, with 95 per cent confidence limits at 97.0 and 114.3 per cent, which indicates that remanence is pre-tilting. The lack of evidence of metamorphism in the section of the Alentuy formation, and the coincidence of the HTC directions in various types of rocks are additional arguments in favour of the primary origin of the HTC. We therefore conclude that the formation mean direction in stratigraphic coordinates ($D_s = 225.2°$, $I_s = -76.2°$; $\alpha_{95} = 8.1°$, $n = 15$ sites; Table 3) is indeed the primary palaeomagnetic direction in the Alentuy formation.

We finally note that the HTC has a reverse polarity direction in almost all of the sites, which is typical for the Late Permian

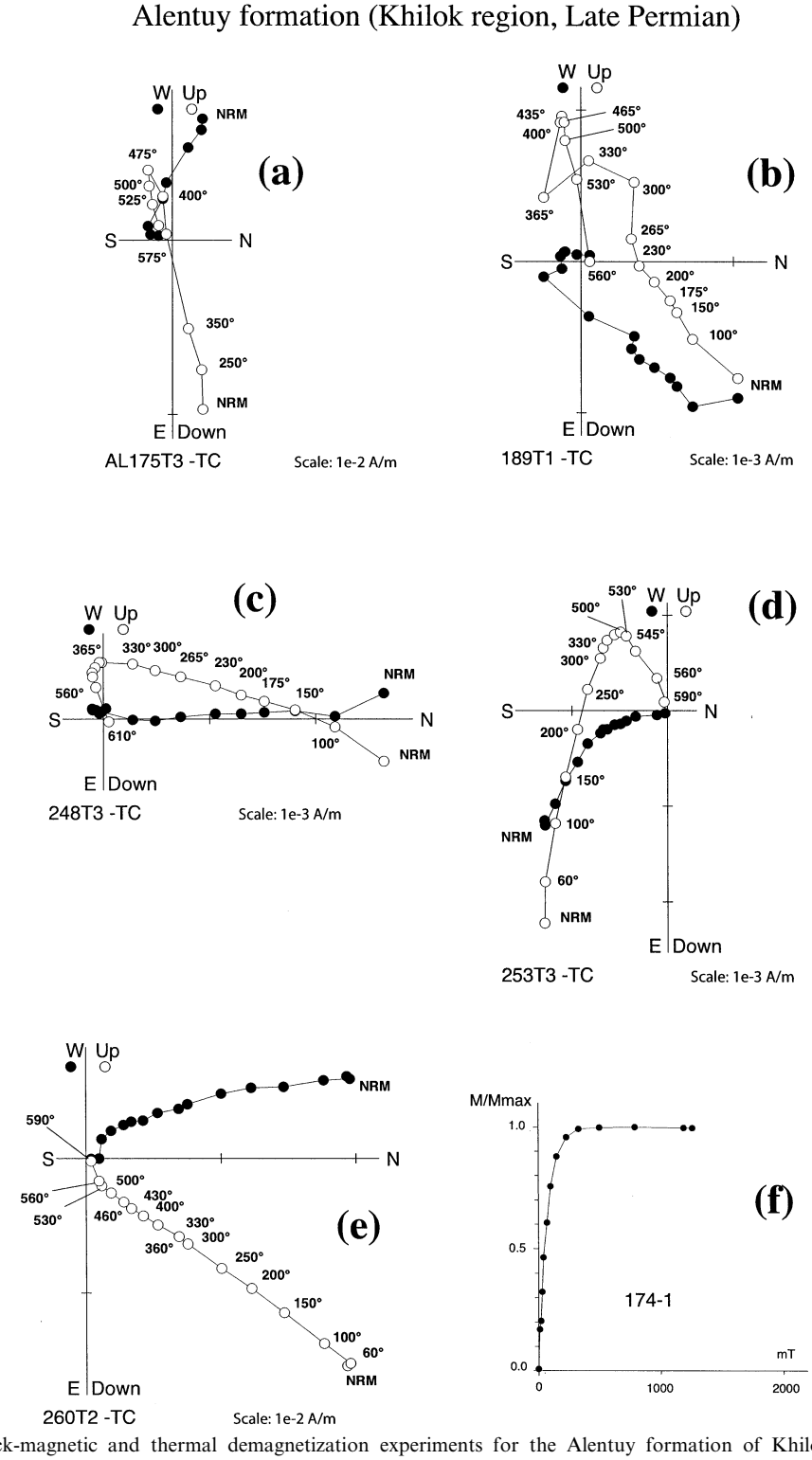

Figure 6. Results of rock-magnetic and thermal demagnetization experiments for the Alentuy formation of Khilok region (Late Permian). (a)–(e) Typical orthogonal vector plots (Zijderveld 1967), in tilt-corrected coordinates, for thermal demagnetizations (steps indicated in °C). Symbols: same conventions as in Fig. 3. (f) IRM acquisition in fields of up to 1.2 T showing the presence of a low-coercivity magnetic mineral.

(reverse Kiaman superchron). Only four samples, out of 10, of site 18-10, which is the uppermost in the sampled formation, display positive magnetic inclinations of the HTC (Fig. 6e). The six samples above these four positive inclination samples again have reverse directions, the same as for all the other sites of the formation. From the data of this site, we assume that most of the Alentuy formation was formed during the Kiaman superchron, with formation ending in the Tatarian (uppermost Permian), during a normal polarity interval. However, we do not have enough evidence for this from the present study.

Table 3. Site-mean palaeomagnetic directions for the high-temperature components for Alentuy formation rocks (Late Permian; location: 50.8°N, 107.2°E).

Site	n	D_g	I_g	D_s	I_s	k	α_{95}	N/R	Notes
17-1	6	225.5	−44.2	–	–	257.6	4.2	R	sandstones
	(6d)	–	–	202.1	−58.4	156.8	5.4		(260/17–274/31)
17-2	6	257.1	−43.1	–	–	28.8	12.9	R	tuff-sandstones
	(5d1cc)	–	–	233.3	−79.3	21.3	15.1		(263/27–274/55)
17-3	5	52.8	−82.8	229.3	−77.2	80.2	8.6	R	tuffs (51/20)
	(5d)								
17-4	10	11.5	−66.3	316.1	−75.4	8.0	18.2	R	tuffs
	(10d)								(51/20)
17-5	5	298.9	−63.7	272.3	−51.9	37.3	13.1	R	tuffs
	(4d + 1cc)								(51/20)
17-6	8	50.4	−76.4	–	–	90.6	6.0	R	fine sindstones
	(5d + 3cc)	–	–	219.0	−83.8	86.5	6.2		(41/18–56/20)
17-7	5	136.8	−76.9	195.1	−66.9	43.5	11.7	R	andesite-dicites
	(5d)								(51/20)
18-1	5	97.3	−38.3	–	–	23.0	17.4	R	sandstones
	(3d + 2cc)	–	–	121.1	−76.9	26.9	16.1	R	(82/38–94/50)
18-2	7	75.7	−47.1	–	–	15.2	16.6	R	sandstones
	(4d + 3cc)	–	–	309.1	−82.0	16.7	15.8		(78/40–91/50)
18-3	6	124.5	−63.1	–	–	37.4	11.9	R	sandstones
	(3d + 3cc)	–	–	225.8	−64.4	31.1	13.1		(83/41–88/50)
18-4	7	98.7	−53.0	–	–	62.4	8.0	R	sandstones
	(4d + 3cc)	–	–	215.1	−74.1	100.9	6.3		(74/32–98/47)
18-5	5	77.2	−52.0	–	–	15.8	19.9	R	sandstones
	(5d)	–	–	339.1	−76.6	36.0	12.9		(91/40–112/54)
18-6	4	150.9	−54.2	–	–	196.9	7.0	R	tuffs
	(3d + 1cc)	–	–	208.1	−69.8	102.7	9.7		(109/30–119/39)
18-8	7	91.2	−63.0	–	–	27.0	11.8	R	flows of
	(7d)	–	–	195.3	−74.8	43.4	9.3		andesite-dicites
									(53/30–87/37)
18-10	10	145.8	−65.4	207.1	−53.4	16.4	12.3	N/R	flows of
	(10d)							(4/6)	andesite-dicites
									(70/35)
	15	109.2	−76.4	–	–	6.8	15.8		
	sites	–	–	225.2	−76.2	23.4	8.1		

Same abbreviations as in Table 1. In the last column, the bedding orientation is marked. For example (260/17–274/31) means that azimuth of dip changes from 260° to 274°, and dip changes from 17° to 31°, for this site. Note that each sample calculations individual azimuth of dip and dip were used.

4.2.2 *The Irkutsk Jurassic basin of the Sibernian platform*

The NRM intensity of the samples from this formation is rather low and ranges from 0.5 to 1.5 mA m^{-1}. However, the thermal demagnetization curves (Fig. 8) show evidence of two components of magnetization in most of the 160 samples. A LTC demagnetizes between NRM and 250–330 °C. The formation mean of this LTC, computed at the site level, averages at $D_g = 354.8°$, $I_g = 69.0°$; $k_g = 55.7°$, $\alpha_{95} = 5.0°$ *in situ*, and $D_s = 0.3°$, $I_s = 70.1°$; $k_s = 32.7°$, $\alpha_{95} = 6.5°$, $n = 16$ after tilt-correction. The k parameter tends to decrease upon unfolding, but, due to the weak dip angles of the bedding plane, this is not significant at the 95 per cent confidence level. However, the *in situ* average conforms to the present-day geomagnetic field direction ($D = 357.7°$, $I = 71.3°$), and we therefore assume that the LTC is a recent overprint.

After removal of the LTC, a weak and often noisy HTC, which is completely unblocked by 550–590 °C (Fig. 8), could be identified. This HTC has either northeast downward directions (Fig. 8a, specimens 39C-J5 and 122B-J6), or southwest upward directions (Fig. 8a, specimen 86B-J11). This component could be resolved in orthogonal plots in only about 30 per cent of the studied specimens. In most cases, the demagnetization path does not converge towards the origin, as shown for specimen 63B-J8 in Fig. 8(b) (right), but aligns along a great circle which, in that case, converges towards an upward direction without reaching it (Fig. 8b, left). This kind of behaviour has been observed in most of the samples having a reverse HTC. In such situations the remagnetzation planes were used, and the combined method for directions and sector constraint (McFadden & McElhinny 1988) was used for calculating the site-mean direction. We note that, although all the polarity changes follow the stratigraphic sequence, reverse polarities could be determined only with the remagnetization circles method.

The site-mean directions of the HTC (Fig. 7b, Table 4) are very scattered, at the site and the formation levels. This dispersion probably arises from the low intensity of the HTC, which could be determined only with the great-circle method in a large number of samples, and is quite noisy in the other cases. Owing to the subhorizontal bedding of these Jurassic rocks from the Siberian platform, the k parameter does not significantly change upon unfolding, and the fold test is inconclusive.

Table 4. Site-mean directions for the high-temperature components for south Siberia platform formations (Early–Middle Jurassic; location: 52.0°N, 104.0°E).

Site	n/N	D_g	I_g	D_s	I_s	k	α_{95}	N/R	Notes
J1	18/21	0.1	78.4	0.1	78.4	2.9	24.6	18/–	16d + 2cc
J2	7/15	254.2	−53.7	254.5	−53.7	5.6	29.3	1/6	3d + 4cc
J3	4/7	234.2	−37.4	234.2	−37.4	4.0	104.7	–/4	4cc
J4	5/8	39.9	75.3	39.9	75.3	2.2	68.2	5/–	4d + 1cc
J5	8/8	8.9	41.1	8.3	29.1	5.4	27.5	2/6	2d + 6cc
J6	8/8	181.7	−61.2	180.5	−67.2	15.8	15.5	3/5	2d + 6cc
J7	8/8	246.4	−40.9	245.8	−49.4	2.5	43.5	2/6	4d + 4cc
J8	7/8	343.2	59.9	343.2	59.2	3.0	42.7	3/4	3d + 4cc
J9	6/8	177.2	−64.7	193.7	−53.3	8.7	26.5	–/6	2d + 4cc
J11	4/8	222.8	−28.0	222.8	−28.0	16.3	31.8	–/4	1d + 3cc
J12	7/8	32.0	56.2	49.3	62.9	4.4	35.4	4/3	1d + 6cc
J13	8/8	25.4	68.1	104.0	73.9	5.5	27.4	3/5	2d + 6cc
J14	7/8	266.7	−66.1	266.7	−66.1	2.8	44.6	–/7	3d + 4cc
J15	6/8	343.4	80.9	343.4	80.9	9.3	25.6	3/3	2d + 4cc
J16	5/7	334.7	62.1	13.7	59.1	9.3	27.1	5/–	4d + 1cc
Mean	15	30.5	62.6	–	–	12.6	11.2		All sites
	sites	–	–	36.3	62.4	12.1	11.5		together
	9	20.1	64.7	–	–	14.3	14.1		Sites with
	sites	–	–	29.5	63.3	11.3	16.0		$\alpha_{95} < 35°$

Same abbreviations as in Table 1.

However, the presence of both polarities, and the fact that the LTC and HTC show different directions, supports the idea that the HTC might be the primary Jurassic magnetization of these rocks. The tilt-corrected HTC, which is $D_s = 29.5°$, $I_s = 63.3°$, $k_s = 11.3$, $\alpha_{95} = 16.0°$, $n = 9$ (Table 4) should, however, be considered as a preliminary rough estimate of the Lower–Middle Jurassic magnetic field of Siberia.

Because of its very large uncertainty, due to the problems in demagnetization given above, the Lower–Middle Jurassic palaeopole of the Irkutsk basin (Table 4) deserves only little attention. We conclude that the magnetization of this series might indeed be primary, because of the presence of two polarities. Only new palaeomagnetic data from Jurassic formations will help to give the Jurassic palaeoposition of Siberia more precisely.

4.2.3 The Late Jurassic Badin formation of Mogzon region (Chita province)

Badin formation rocks are characterized by the following values of magnetic parameters: NRM = 0.35–0.9 mA m^{-1}, magnetic susceptibility $\chi = 7.0$–8.0×10^{-6} SI units, and $Q = 0.1$–0.2. Both thermal and AF demagnetizations (Fig. 9) resolve two magnetization components. A first, low-temperature component in thermal demagnetization is isolated between NRM and 250 °C. Its average direction in *in situ* coordinates is $D_g = 2.2°$, $I_g = 76.2°$; $k = 78.9$, $\alpha_{95} = 4.7°$, $n = 13$ sites. This component direction is close to the present-day geomagnetic field direction in the region ($D = 353.5°$, $I = 70.5°$), and we consider that this is the present-day overprinting direction.

The high-temperature component is isolated in the temperature range 250–590 °C in the samples of a first group of nine sites (sites 3-1 to 8-3; Fig. 9a, Table 5). In this group of specimens, the HTC component could be isolated by AF demagnetization up to 100 mT (Fig. 9b, left). IRM acquisition curves (Fig. 9c, left) for specimens from this group evidence a presence of low-coercivity minerals. In the second group of three sites (sites 9-1 to 9-3; Table 5, Fig. 9b, right) the HTC was resolved between 200 and 690 °C. IRM experiments (Fig. 9c, right) give curves typical of high-coercivity minerals. From these unblocking temperature ranges and the IRM experiment results, the carrier of the HTC magnetization for the first group of nine sites is probably magnetite, and for the second group could be haematite. Regarding the directions, all the samples from sites 3-1 to 8-3 have a HTC with negative steep upward inclinations, whereas the HTC from all the specimens from sites 9-1 to 9-3 have positive intermediate inclinations.

Thus, we have two very distinct groups of samples, with different unblocking temperature ranges, different magnetic carriers, and distinct magnetization directions. As noted above, sites 9-1 to 9-3 are separated from the other nine sites by faults and a rhyolite intrusion, and have been dated by lateral facies correlation (Likhanov 1991). Moreover, the reversal test (McFadden & McElhinny 1990) appears negative for the tilt-corrected population. We therefore conclude that the magnetizations from groups 3-1 to 8-3 and 9-1 to 9-3 may have a different age, and this is the reason why we computed the formation mean directions for each group separately (Table 5).

The population of site-mean directions of sites 3-1 to 8-3 tends to cluster upon unfolding (Table 5, Fig. 8c). In effect, the precision parameter k is higher in stratigraphic coordinates ($k_s = 167.7$) than in geographical coordinates ($k_g = 49.6$). This difference ($k_s/k_g = 3.38$) is significant at the 95 per cent confidence level, with the critical value of the confidence level 2.33. We therefore assume that the HTC may be the primary magnetization for, at least, this group of sites. The fold test of Watson & Enkin (1993) gives an optimum degree of untilting (50 percentile, 1000 trials) at 97.3 per cent (with 95 per cent confidence limits at 75.5 and 120.0 per cent). This estimate is very near 100 per cent and indicates that remanence is indeed pretilting.

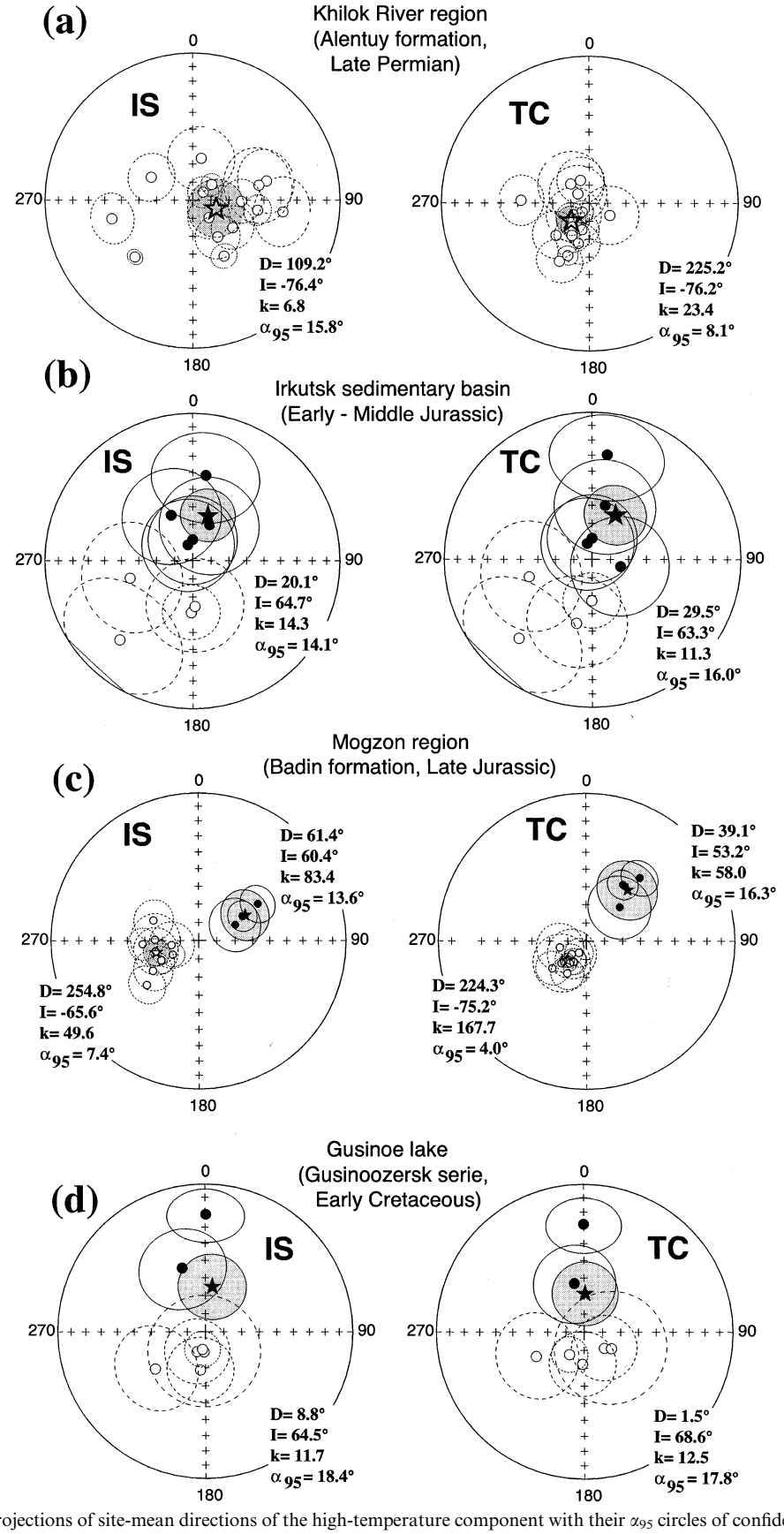

Figure 7. Equal-area projections of site-mean directions of the high-temperature component with their α_{95} circles of confidence shown in *in situ* (left) and tilt-corrected (right) coordinates, for (a) Khilok river region (Alentuy formation, Late Permian); (b) Siberian platform Early–Middle Jurassic sediment field; (c) Mogzon region (Badin formation, Late Jurassic); (d) Gusinoe Ozero Depression (Gosinoozersk series, Early Cretaceous). Closed (open) symbols: downward (upward) inclinations. Star: formation mean directions.

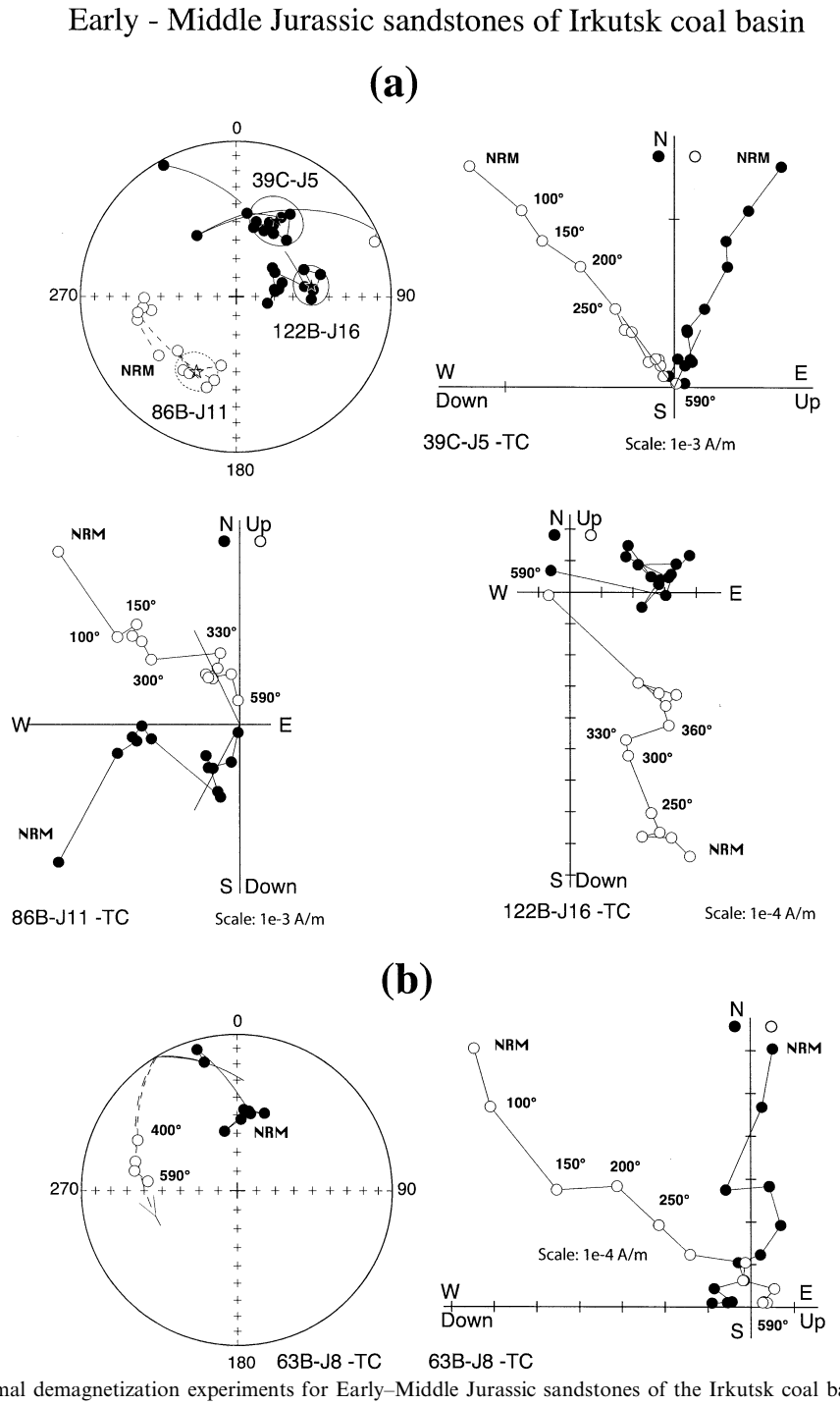

Figure 8. Results of thermal demagnetization experiments for Early–Middle Jurassic sandstones of the Irkutsk coal basin, shown in orthogonal vector projections (same conventions as in Fig. 3) and in stereonets. (a) Plots illustrate the presence of normal and reverse polarities. (b) Plots illustrate the great-circle evolution of magnetization.

The interpretation of the HTC from the remaining three sites 9-1 to 9-3 (separate from previous sites locality) is less easy. The precision parameter k does not change upon unfolding, the magnetic mineralogy appears to be different from the previous group, and, being established only on facies correlations, the age of the rocks is not well constrained. We thus believe that these directions could be a remagnetization, or, alternatively, a primary magnetization of rocks of a different age. Because of these uncertainties, we neglect these three site-mean directions in further discussion.

4.2.4 *The Early Cretaceous formations of Gusinoe lake*

The collection of studied Cretaceous rocks mostly consists of grey and yellow sandstones and siltstones of different grain sizes. The intensity of the NRM is very low and ranges from 0.7 to 2.3 mA m^{-1}. Magnetic susceptibility also shows low values, from 5 to 20×10^{-6} SI units. During thermal demagnetization, the magnetic susceptibility remained stable for the samples from sites K17–K18, K23–K25, and K27–K28, whereas it showed a large increase starting at 360–400 °C for the samples from sites

Table 5. Site-mean palaeomagnetic directions for the high-temperature components for Badin formation rocks (Late Jurassic; location: 51.8°N, 112.0°E).

Site	n	D_g	I_g	D_s	I_s	k	α_{95}	N/R	Notes
3-1	6	266.5	−58.6	220.5	−76.8	65.1	8.4	R	6d
3-2	8	256.4	−65.3	–	–	21.0	12.6	R	6d + 2cc
		–	–	228.2	−71.8	13.7	15.8		
3-3	7	293.9	−62.4	–	–	30.6	11.1	R	7d
		–	–	227.9	−79.4	21.1	13.5		
3-4	6	242.1	−73.7	–	–	105.3	6.6	R	6d
		–	–	210.9	−76.9	90.2	7.1		
4-1	9	271.3	−65.6	–	–	14.6	13.9	R	9d
		–	–	256.3	−75.2	16.5	13.1		
4-2	9	261.1	−74.7	–	–	17.6	12.6	R	9d
		–	–	211.3	−82.5	44.4	7.8		
8-1	10	242.9	−66.6	–	–	44.3	7.3	R	10d
		–	–	231.3	−66.1	28.4	9.2		
8-2	6	229.9	−51.8	–	–	43.8	10.2	R	6d
		–	–	216.4	−74.9	263.6	4.1		
8-3	7	237.1	−59.5	–	–	31.5	10.9	R	7d
		–	–	210.4	−69.5	46.4	9.0		
9-1	5	61.1	62.2	33.3	52.4	87.2	8.2	N	5d
9-2	6	66.9	68.0	–	–	22.7	14.4	N	6d
		–	–	44.9	63.5	16.0	17.2		
9-3	7	58.4	51.0	40.5	43.3	39.9	9.9	N	5d + 2cc
3-1 – 8-3	9 sites	254.8	−65.6	–	–	49.6	7.4	–/9	only reverse polarity sites
		–	–	224.3	−75.2	167.7	4.0		
9-1 – 9-3	3 sites	61.4	60.4	–	–	83.4	13.6	4/–	only normal polarity sites
		–	–	39.1	53.2	58.0	16.3		

Same abbreviations as in Table 1.

K19–K22, and K26. The IRM experiments (Fig. 10c) show the presence of low-coercivity minerals, which saturate in magnetic fields of 0.15–0.3 T. A Curie point experiment was conducted in the palaeomagnetic laboratory of Kazan State University on equipment and with the method described in Burov *et al.* (1986). A Curie temperature of 585–590 °C was obtained. Thus, both IRM and Curie-temperature experiments argue for the presence of magnetite.

The thermal demagnetization (Figs 10a and b) isolated a LTC in almost all of the studied samples. This LTC unblocks between room temperature and 250–300 °C, and has systematically normal, northward and down, directions. It averages at $D_g = 21.3°$, $I_g = 73.1°$; $k_g = 73.3°$, $\alpha_{95} = 5.1°$, $n = 12$ sites in *in situ* coordinates, and the k parameter decreases to $k_s = 29.0$ upon unfolding. The fold test (McElhinny 1964) is negative at the 95 per cent confidence level, and we therefore conclude that this LTC is a post-folding remagnetization. However, this mean direction is significantly different from the present-day geomagnetic field in the sampling area ($D = 356.4°$, $I = 70.5°$).

Following this LTC, a weak HTC demagnetizes in temperatures of up to 590 °C (Fig. 10). It may have either normal (specimen 200B-K25, Fig. 10a) or reverse (specimen 132B-K17, Fig. 10a) polarity. The most common behaviour, encountered in half of the specimen collection, is illustrated in Fig. 10(b), specimen 217B-K27, in which the demagnetization path does not converge towards the origin of the orthogonal plot, but tends to align along a great circle. This attests to the presence of at least two components with overlapping temperature spectra. In that case, the remagnetization planes were used to determine the site-mean HTC directions (Table 6) using the McFadden & McElhinny (1988) method. Finally, about 30 per cent of the treated specimens did not allow the HTC to be determined, because of noisy ends of demagnetizations.

As a consequence of difficulties in isolating the HTC, the site-mean directions of this component (Table 6, Fig. 7d) generally show a large scatter at both site and formation levels. Excluding sites K20, K23, K24 and K26, where α_{95} is larger than 35°, this component averages at $D_g = 8.8°$, $Ig = 64.5°$; $kg = 11.7$, $\alpha_{95} = 18.4°$, $n = 7$ in *in situ* coordinates, and $D_s = 1.5°$, $I_s = 1.5°$; $k_s = 12.5$, $\alpha_{95} = 17.8°$, $n = 7$ after tilt-correction. The ratio of precision parameters is $k_s/k_g = 1.07$, and the fold test is therefore inconclusive. We finally note that these average directions in either geographical or stratigraphic coordinates are not distinguishable from the LTC average direction given above.

Owing to the lack of any fold test, and to the very large scatter of HTC directions, arising from difficulties in isolating this HTC, the palaeopole of the Gusinoe lake Early Cretaceous formation cannot be obtained reliably. In effect, its very large *dp*/*dm* ellipse of confidence encompasses all the poles of the reference Eurasian APWP from the present-day to 200 Ma. We therefore conclude that we failed in constraining the time of closure of the Mongol–Okhotsk Ocean with the palaeomagnetic study of this formation.

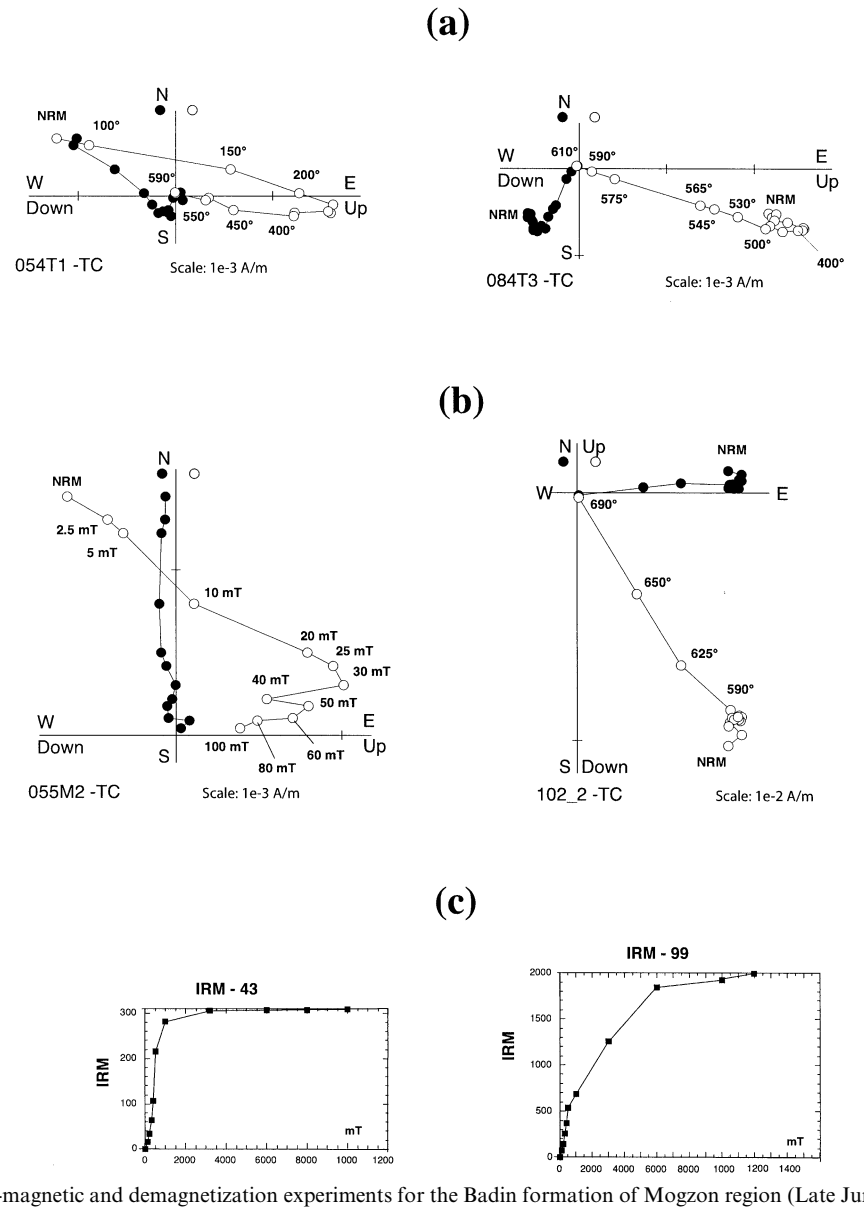

Figure 9. Results of rock-magnetic and demagnetization experiments for the Badin formation of Mogzon region (Late Jurassic). (a) and (b) Typical orthogonal vector plots (Zijderveld 1967), in tilt-corrected coordinates, for thermal (steps indicated in °C) and AF (steps indicated in mT) demagnetizations. Symbols: same conventions as in Fig. 3. (c) IRM acquisition in fields of up to 1.2 T showing the presence of both low-coercivity (left, sample 43) and high-coercivity (right, sample 99) magnetic minerals.

5 DISCUSSION

The palaeomagnetic analysis presented above enables two magnetization components to be separated in each of the six localities studied. The LTC shows negative fold tests in two formations (Late Permian Alentuy and Early Cretaceous Gusinoe lake formations), and, because of flat-lying or monoclinal bedding attitude, inconclusive fold tests in the four other localities. In every case, this LTC in geographical coordinates is parallel, or very close, to the present-day geomagnetic field direction at the sampling places. We therefore assume that the LTC is a present-day, or recent, remagnetization. After this component, a HTC could be identified in most of the samples. This HTC was not always easy to separate from the LTC, because of overlapping unblocking temperature spectra and/or weak intensity. As a consequence, the HTC formation mean directions at some localities are determined with low accuracy or confidence (e.g. Low–Middle Jurassic Irkutsk basin formation, Gusinoe lake formation), and these directions should be considered as preliminary results. Because of the monoclinal attitude of bedding planes at several localities, the fold test is positive only in the Late Permian Alentuy formation, and in the Late Jurassic Badin formation (only for reversal directions). The fold test is inconclusive in the Jurassic formations of Shadaron and the Irkutsk basin, and the Cretaceous Gusinoe lake formation. In the Late Permian Belektuy formation, the

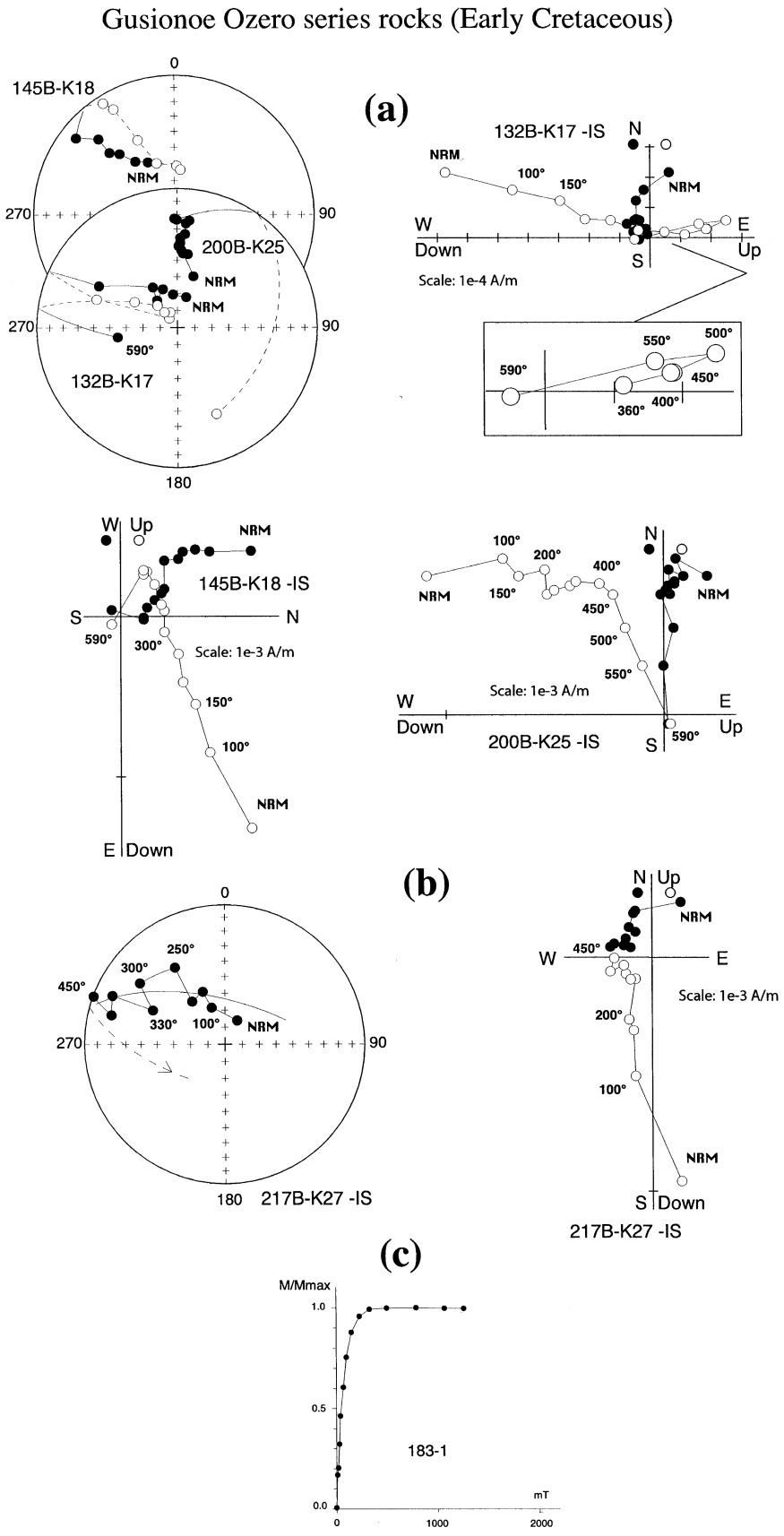

Figure 10. Results of rock-magnetic and thermal demagnetization experiments for the Gusionoe Ozero formation (Early Cretaceous), shown in orthogonal vector projections (same conventions as in Fig. 3) and in stereonets. (a) Plots illustrate the presence of normal and reverse polarities. (b) Plots illustrate the great-circle evolution of magnetization. (c) IRM acquisition in fields of up to 1.2 T showing the presence of a low-coercivity magnetic mineral.

Table 6. Site-mean directions for the high-temperature components for Gusinoe Ozero formations (Early Cretaceous; location: 51.2°N, 106.48°E).

Site	n/N	D_g	I_g	D_s	I_s	k	α_{95}	N/R	Notes
K17	9/10	203.1	−78.1	128.5	−75.9	10.2	18.0	R	2d + 7cc
K18	6	183.9	−78.9	121.1	−72.6	5.6	31.3	R	5d + 1cc
K19	7	187.6	−68.6	183.1	−72.3	12.8	18.2	3/4	4d + 3cc
K20	3/7	196.2	−73.3	192.0	−77.1	13.2	–	R	3cc
K21	7	189.8	−80.2	213.3	−75.3	55.6	9.9	R	7cc
K22	4/7	233.4	−55.1	243.1	−60.2	57.9	23.4	R	4cc
K23	3/7	236.0	−72.6	268.7	−57.7	29.4	–	R	3cc
K24	4/7	177.7	−70.1	202.6	−74.7	5.1	60.5	R	1d + 3cc
K25	3/7	0.4	21.7	359.9	28.0	132.2	17.8	N	1d + 2cc
K26	3/6	309.8	56.2	287.3	64.2	106.7	67.9	N	3cc
K27	6	340.1	52.1	–	–	9.9	23.2	N	4d + 2cc
		–	–	348.8	62.5	10.8	22.1		
Mean	11	4.6	67.7	–	–	14.5	12.4		All sites
	sites	–	–	6.3	72.9	12.6	13.4		together
	7	8.8	64.5	–	–	11.7	18.4		Sites with
	sites	–	–	1.5	68.6	12.5	17.8		$\alpha_{95} < 35°$

Same abbreviations as in Table 1.

conventional fold test is not positive, but the Watson & Enkin (1993) test is.

Finally, we note that the formation mean HTCs are not parallel to the present-day geomagnetic field direction in four of the six formations studied (the Late Permian Belektuy formation, the Late Permian Alentuy formation, the Middle–Late Jurassic Shadaron formation, and the Late Jurassic Badin formation). Both normal and reverse polarity HTCs could be identified in every locality. We therefore make the assumption that these HTCs are the primary palaeomagnetic directions of the four formations studied (the Late Permian Belektuy formation, the Late Permian Alentuy formation, the Middle–Late Jurassic Shadaron formation, and the Late Jurassic Badin formation). The corresponding palaeopoles, computed after tilt-corrected magnetization directions, are listed in Table 7, along with selected palaeopoles from the literature for Siberia, Eurasia, North China and Tarim. In the following, we discuss these palaeopoles with respect to the reference APWPs of Eurasia (Besse & Courtillot 1991; Van der Voo 1993), North China (NCB; Zhao *et al*. 1996; Enkin *et al*. 1992; Gilder & Courtillot 1997), and Inner Mongolia (Zhao *et al*. 1990).

5.1 Permian

The Late Permian palaeopole of the Alentuy formation (Fig. 11, Table 7), from the north of the Mongol–Okhotsk suture, is very close to the Jurassic part of the Eurasian APWP. However, the small circle passing through this pole, and centred on the site location, cuts the Permian part of the Eurasian APWP. We therefore have two possibilities: either this formation was remagnetized in the Jurassic, or its magnetization is the primary Late Permian magnetization, and the sampling area has undergone a counterclockwise rotation around a local vertical axis. We note, however, that the magnetizations of this formation pass a positive fold test, and large local rotations have already been found by Pruner (1992), Kravchinsky (1995), and Halim *et al*. (1998a). Halim *et al*. (1998b) proposed that, in the vicinity of the Mongol–Okhotsk suture and Trans-Baikal area, these rotations are due to a left-lateral megashear along the Mongol–Okhotsk suture which allows eastward extrusion of Mongolia with respect to Siberia, under the effect of the penetration of India into Eurasia. For these reasons, we conclude that the Alentuy formation palaeopole is most likely a counter-clockwise-rotated Late Permian palaeopole (the rotation angle between Alentuy area with respect to the reference Eurasian palaeopole is $28.7° \pm 24.7°$), and thus consistent with the reference Eurasia APWP, and characterizes the palaeoposition of the Siberia block in Late Permian times. The palaeolatitude difference from the reference Eurasian Late Permian (240–260 Ma) palaeomagnetic pole is $0.2° \pm 10.6°$.

The Belektuy formation is situated south of the Mongol–Okhotsk suture, in the Amuria block as defined by Zonenshain *et al*. (1990). In contrast to the Alentuy palaeopole, the Late Permian palaeopole of the Belektuy formation (Fig. 11, Table 7; this study) is largely inconsistent with the Permian parts of both the Eurasian and NCB APWP. However, it is consistent with the Middle–Late Carboniferous Kharabishir and the Early Permian Zhipkoshin palaeopoles (Table 7; Xu *et al*. 1997) of the same region, and the small circle centred on the Belektuy location and passing through its palaeopole (Fig. 11) contains the Middle–Late Carboniferous to Late Permian part of the NCB APWP. The palaeolatitude difference from the NCB reference Late Permian palaeomagnetic pole is $5.2° \pm 13.0°$. This small circle also passes near the Late Carboniferous and Early Permian palaeopoles from Inner Mongolia (Pruner 1992). Thus we conclude that, except for large rotations about local vertical axes, these palaeopoles are consistent with the Late Carboniferous to Late Permian part of the APWP of NCB. The large palaeolatitude difference ($42.9° \pm 16.7°$, after Table 7) between the Alentuy and the Belektuy locations provides evidence of the presence of an ocean between these two places.

This conclusion could appear to somewhat contradict the estimates of Zonenshain *et al*. (1990) of the age of the collision between Amuria and Siberia. In effect, based on the age of metamorphism and intraplate magmatism from the Mongolian Khingayn Mountains, these authors date the collision as Late

Table 7. Palaeozoic and Mesozoic palaeopoles from the present study, and selected palaeopoles from Siberia, Eurasia, North China and Tarim.

Pole	Block/Area	Formation	Age	Site Lat	Lon	Palaeopole Lat	Lon	*dp/dm* (A_{95})	N	Palaeolat.	References
Siberia and **Trans-Baikal**											
1. North of M-O suture											
1	Khilok	Alentuy fm.	P2	50.8	107.2	63.1	151.0	13.8/15.0	15S	63.8	Kravchinsky (1995), Kuzmin & Kravchinsky (1996) and this study
2	Lena river	sediments, no details	T2–3-J1	72.6	124.7	47	129	4/16	26 s	64.3	Pisarevsky (1982)
3	Ilek	Ilek group	J2–3	56.5	89.5a	74	135	10.4/11.2	101 s	65.3	Pospelova *et al.* (1971)
4	Mogzon	Badin fm.	J3	51.8	112.0	64.4	161.0	6.7/7.3	9S	62.1	Kravchinsky (1995), Kuzmin & Kravchinsky (1996) and this study
5	Kondersky	intrusives,	J+K sediments	57.7	134.6	75	163	10.4/10.9	34 s	69.7	Pavlov (1993)
2. South of M-O suture											
6	Chiron	Karashibir fm.	C2 (320–296)	51.53	115.39	10.2	186.2	14.8	8S	19.9	Xu *et al.* (1997)
7	Chiron	Zhipkhoshin fm.	P1	51.53	115.39	33.8	207.8	26.3	5S	24.4	Xu *et al.* (1997)
8	Borzja	Belektuy fm.	P2	50.65	116.88	8.3	183.9	9.5/16.2	14S	20.9	Kravchinsky (1995), Kuzmin & Kravchinsky (1996), Xu *et al.* (1997) and this study
9a	Unda-Daya	Shadaron fm. (tilt-corrected)	J2–3	51.5	117.5	59.6	279.0	3.2/5.4	8S	22.1	This study
9b	Unda-Daya	Shadaron fm (tilt-corrected)	J2–3	51.5	117.5	68.6	261.8	3.4/4.9	8S	33	This study
Inner Mongolia											
10		–	J3	–	–	68.5	231.6	9.5	4 L		Zhao *et al.* (1990)
11		–	P2	–	–	52.5	342.4	6.4	12 L		Zhao *et al.* (1990)
12		–	C3	–	–	32.6	338.1	4.4	29 L		Zhao *et al.* (1990)
Eurasia (APWP)											
10		–	J3	–	–	70.0	157.8	6.6	7 L	–	Besse & Courtillot (1991)
11		–	J2	–	–	78.5	178.7	3.9	16 L	–	Besse & Courtillot (1991)
12		–	J1	–	–	78.5	178.7	3.9	12 L	–	Besse & Courtillot (1991)
North China											
13		–	J3	31.6	116.0	74.4	222.8	5.9	10 L	26.0	Gilder & Courtillot (1997)
14		–	J2	34.0	112.5	73.6	249.3	4.9	23 L	21.5	Gilder & Courtillot (1997)
15		–	J1	36.2	109.3	82.4	286.0	10.0	10 L	28.6	Yang *et al.* (1992)
Tarim											
16		–	P2-T1	42.1	83.3	71.8	187.6	5.5/7.8	16S	35.4	McFadden *et al.* (1988)
17		–	J3-K1	42.0	81.6	64.6	208.9	9.0	6 L	24.3	Li *et al.* (1988)

Lat (Lon): latitude (longitude) of sampling sites or palaeomagnetic poles; A_{95}: radius of the 95 per cent confidence circle of the virtual palaeomagnetic pole; *dp/dm*: semiaxes of the confidence circle of palaeomagnetic pole; Palaeolat.: palaeolatitude; N: number of localities or sites (L), samples (s) or sites (S) used to determine the pole.

Carboniferous–Early Permian for the western part of Amuria. We may therefore suspect a 'scissor-like' closure of the Mongol–Okhotsk Ocean, beginning at the end of the Carboniferous in the west. Our data would therefore suggest a remaining large oceanic gap between Amuria and Siberia in the Late Permian, at the longitude of the Belektuy sites.

The very large rotation of the Belektuy, Karabishir and Zhipkoshin palaeopoles with respect to the west Amuria (or Inner Mongolia) poles (Pruner *et al.* 1992) may result from at least three different but overlapping mechanisms.

(1) According to Zonenshain *et al.* (1990), the formation of the Amuria block results from the amalgamation of a number of microblocks (Khangay, Khentey, Central-Mongolian, Argun, Khingan-Bureya) in the Palaeozoic. Part of the rotations just described could have arisen at the end of this history, from relative movements of these microblocks.

(2) The post-Late Permian collision of Amuria and Siberia could probably produce significant local rotations.

(3) The suspected large left-lateral Tertiary shear along the Mongol–Okhotsk suture proposed by Halim *et al.* (1998b) provides a further possible mechanism for large rotations.

Because of these large rotations of our Belektuy pole, and Karabishir and Zhipkoshin palaeopoles (Xu *et al.* 1997), the width of the Mongol–Okhotsk Ocean in Late Permian times is not easy to assess, but could be several thousands of kilometres. In effect (Table 7), the palaeolatitude difference between

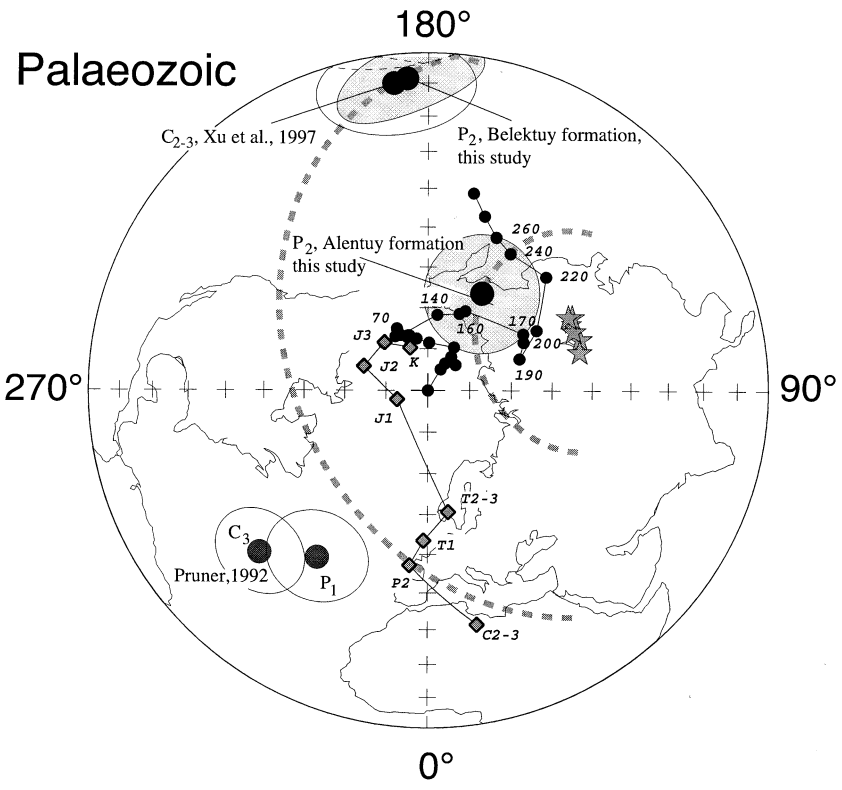

Figure 11. Equal-area projection of the northern hemisphere of the Carboniferous and Permian palaeopoles (large dots with *dp*/*dm* ellipses of confidence) from the present study (Belektuy and Alentuy formations), and from the literature (Pruner 1992; Xu *et al*. 1997). Small black dots: Eurasian APWP (Besse & Courtillot 1990; Van der Voo 1993) with ages indicated in Ma. Diamonds: North China Block (NCB) APWP (Enkin *et al*. 1992; Gilder & Courtillot 1997). Dotted curves are the small circles passing through our Permian poles and centred on site locations (grey stars).

our Alentuy and Belektuy formation localities amounts to $\Delta_{\text{palaeolat}} = 42.9^\circ \pm 16.7^\circ$ (4750 km ± 1850 km), whereas their present-day latitude difference is $\Delta_{\text{lat}} = 0.2^\circ$.

5.2 Jurassic

The Late Jurassic palaeopole from the Badin formation situated north of the Mongol–Okhotsk suture (Fig. 12, Table 7) appears quite consistent with the 150–160 Ma poles of the reference APWP for Eurasia (Besse & Courtillot 1991). In effect, the small circle centred on site locations and passing through the Badin palaeopole contains the 150 and 160 Ma poles of the APWP. This demonstrates a slight clockwise rotation of the Mogzon locality with respect to Siberia, although in limits of confidence this rotation is not significant. We therefore conclude that the HTC we have isolated in the Badin formation is indeed the primary magnetization of the formation, and that the corresponding palaeopole may characterize the Late Jurassic palaeoposition of Siberia.

In contrast, the Shadaron Middle–Late Jurassic palaeopole, calculated in tilt-corrected coordinates, from the Amuria microcontinent is largely discordant from the reference APWPs both of Eurasia and of the NCB (Fig. 12). This denotes a possible difference of palaeopositions of the Amuria and North China blocks, the reason for which is not fully clear, but could arise from the fact that the so-called Amuria block was not fully consolidated by that time (Zonenshain *et al*. 1990). However, if we retain the hypothesis that the magnetization of Shadaron rocks is indeed primary, the small circles passing through the Shadaron and Badin formation tilt-corrected palaeopoles (Fig. 12) provide an estimate of the Middle–Late Jurassic palaeolatitude differences between these localities. From Table 7, these difference amount to $\Delta_{\text{palaeolat}} = 40.0^\circ \pm 8.1^\circ$ (4400 ± 900 km) between the Shadaron and Badin localities for a present-day latitude difference of $\Delta_{\text{lat}} = 0.3^\circ$. Although they cannot be directly translated in terms of the width of the Mongol–Okhotsk Ocean in the Middle–Late Jurassic, because this also depends on the relative orientation of the Siberia and Amuria blocks at that time, these palaeolatitude differences point to the remaining large distances between these localities in the Jurassic. This could reflect a rapid north–south convergence of Amuria block localities towards the Siberia block at the end of the Jurassic.

From another angle, if the Shadaron pole is calculated in *in situ* coordinates (68.6°N, 261.8°E, *dp*/*dm* = 3.4°/4.9°), one can see that the difference between the formation palaeolatitude position (33° ± 3.4°) and Inner Mongolian Late Jurassic pole of Zhao *et al*. (1990) is within the confidence limits (Fig. 12, Table 7). The expected palaeolatitude for the Shadaron formation calculated from the Inner Mongolian (INM) pole is 39.4° ± 9.5° (i.e. $\Delta_{\text{palaeolat}} = 6.4^\circ \pm 7.6^\circ$ (710 ± 840 km). In this case, the difference between Shadaron and Badin localities is $\Delta_{\text{palaeolat}} = 29.7^\circ \pm 3.3^\circ$ (3300 ± 360 km). Thus we may raise the question of bedding orientation for andesite and basalt rocks in the Unda-Daya depression. Can this orientation of andesites and basalts be accepted for the whole area from the measuring of sedimentary planes or do some volcanic structures cut the sediments and have a different orientation?

Any of these interpretations matches the idea that the Mongol–Okhotsk Ocean had closed by the beginning of the Cretaceous,

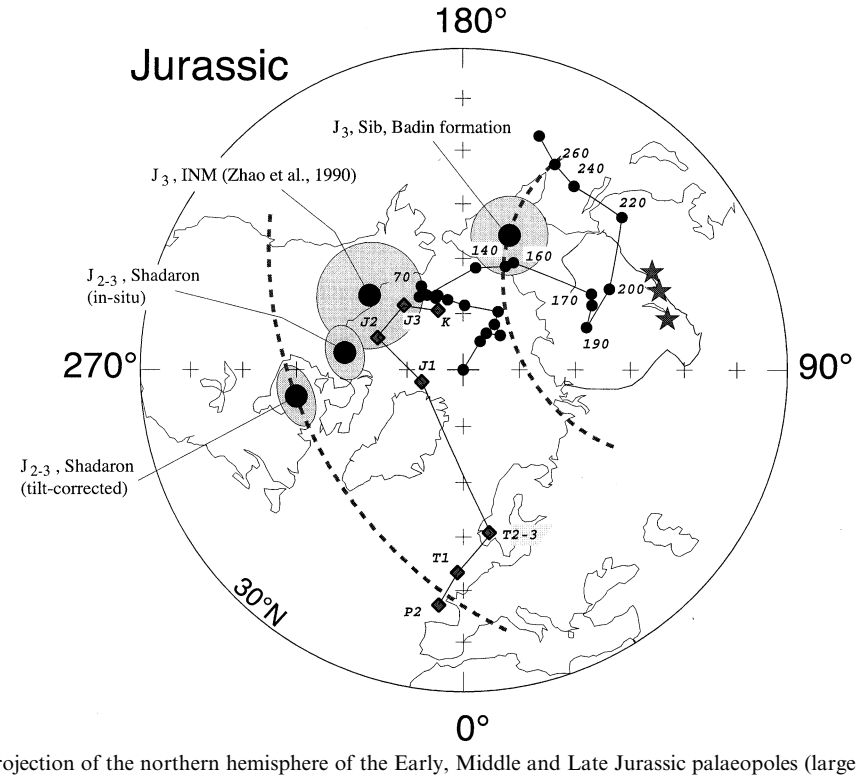

Figure 12. Equal-area projection of the northern hemisphere of the Early, Middle and Late Jurassic palaeopoles (large dots with *dp*/*dm* ellipses of confidence) from the present study. Small dots, diamonds, stars and dotted curves are as in Fig. 11. INM: Inner Mongolia block. Sib: Siberia.

as suspected from the comparison of palaeomagnetic data from the NCB with the Eurasian APWP (e.g. Besse & Courtillot 1991; Enkin *et al*. 1992; Yang *et al*. 1992) and Inner Mongolian poles (Zhao *et al*. 1990). However, there is no geological evidence for the existence of an oceanic space in the Transbaikal region by the Jurassic. We thus propose that shallow intracontinental sedimentary basins, subsequently shortened and folded in the continuing process of the Siberia–China convergence, separated the Amuria block from Siberia. Owing to the very limited number of poles from this region and the large rotations of blocks in the Mongol–Okhotsk suture region, this interpretation is indeed tentative, and should be checked by further palaeomagnetic studies of Jurassic and Cretaceous formations from both sides of the Mongol–Okhotsk suture. Zhao *et al*. (1990) published a number of Late Jurassic poles from Inner Mongolia, which may characterize the Amuria block (Table 7, Fig. 12). Their mean pole is based on four localities (23 sites with 110 samples), where tuff and andesite are present. The closest locality is 200 km south of the Shadaron area. The site-mean directions pass fold and reversal tests, and the mean age from K–Ar dating is 155 Ma. The mean INM Late Jurassic pole implies no significant difference between Amuria and North China. For this reason we consider that our Shadaron pole should be regarded only as a preliminary result from the northern part of Amuria, as it does not fit (in tilt-corrected coordinates) the more reliable pole from Zhao *et al*. (1990).

5.3 The Mongol–Okhotsk Ocean in the Permian and the Jurassic

From the above discussion, we propose the schematic palaeoreconstructions of Eurasia, Tarim, Amuria and the NCB given in Fig. 13, for Middle–Late Permian and Middle–Late Jurassic times. In these reconstructions, Eurasia has been placed according to our new data from the Alentuy formation for the Permian, and from the Badin formation for the Jurassic. These palaeopositions are consistent with the APWP of Eurasia (Besse & Courtillot 1991; Van der Voo 1993), and with the palaeolatitudes from previous good quality data from Siberia for the Jurassic (Pospelova 1971; Pisarevsky 1982; Table 7) and the Carboniferous–Permian (Xu *et al*. 1997). Siberian poles have demagnetization code 2 after the McElhinny & Lock (1996) classification (i.e. AF and thermal demagnetizations), and were obtained directly on the Siberian platform, which excludes any relative rotations. The palaeolatitude of the Tarim block is well constrained by two studies of Gilder *et al*. (1996) and Li *et al*. (1988). In our Middle–Late Permian reconstruction (Fig. 13b), the relative position of Tarim and Eurasia has been constructed after Gilder *et al*. (1996). The palaeoposition of the Amuria microcontinent has been drawn after the palaeolatitude of the Belektuy formation (for the Permian) and the Inner Mongolian pole (for the Jurassic; Zhao *et al*. 1990). As we did not finally solve the problem of our Shadaron tilt-corrected or *in situ* pole, we use the INM pole (Zhao *et al*. 1990) to reconstruct the palaeoposition of Amuria in the Late Jurassic. Because of the large rotations of the sampling localities, the origin of which is not easy to discern, as discussed above, the orientation of the northern margin of the Amuria block is not constrained at all. For the same reason, and because our new poles from Amuria together with the INM pole are all consistent with the NCB APWP, we did not attempt to detail the relative evolution between these two blocks, and left them attached rigidly in the reconstructions.

In the Late Permian (Fig. 13b), the (present-day) southern margin of Eurasia has a meridional orientation. According to our pole from the Belektuy formation, the Amuria (and NCB)

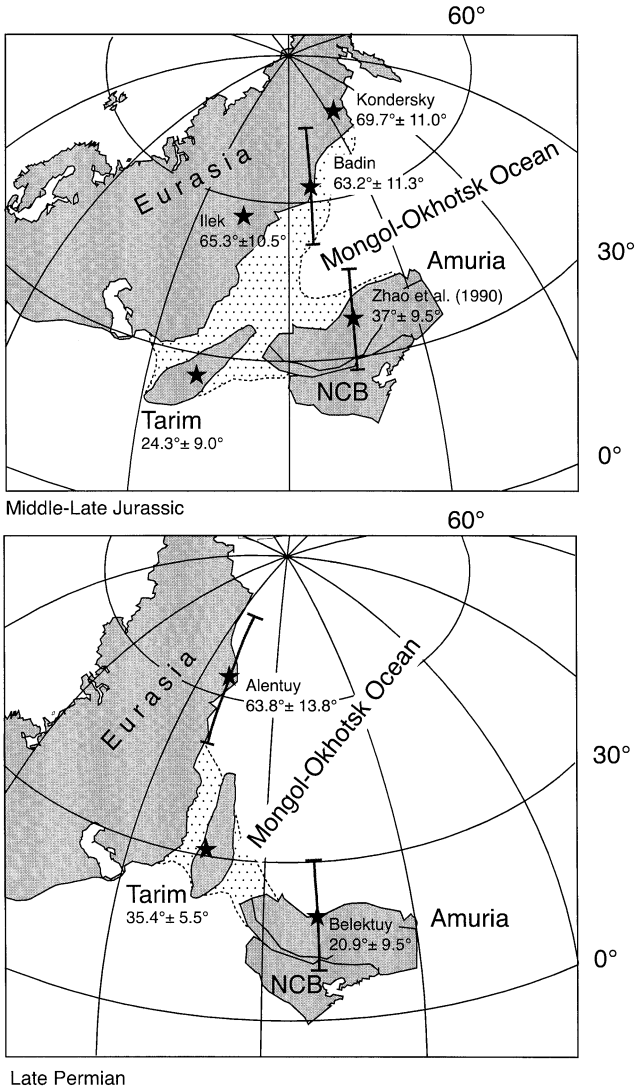

Figure 13. Highly schematic reconstructions of the Mongol–Okhotsk ocean in the Late Permian 1(b) and Middle–Late Jurassic 1(a) based on palaeomagnetic data from Table 7. Black stars: palaeomagnetic sampling locality (except for the Tarim Block, where it represents an arbitrary reference point within the block). Palaeolatitudes with confidence intervals are indicated. For the Jurassic we have shown the possible dry land (dotted area) between Eurasia and the Chinese block to explain the geological data, which suggest a Jurassic closure of the Mongol–Okhotsk Ocean in the west Trans-baikalia region. Our data suggest a still large palaeolatitude difference between the Amuria and Siberia blocks. This difference probably arises both from collision processes and from a left-lateral shear movement along the suture zone, due to the eastward extrusion of Mongolia under the effect of the movement of India into Asia. Error bars α_{95} are shown near localities with their palaeolatitude values.

block is situated much more to the south than the Trans-Baikal region, characterized by our Alentuy pole. This demonstrates the existence of the Mongol–Okhotsk Ocean at that time. Because of the lack of marine sediments of Late Carboniferous and Permian ages, and based on the age of granitoids of the Mongolian Khingay Mountains, Zonenshain *et al.* (1990) proposed that collision between Amuria and Eurasia began in the Late Carboniferous–Early Permian, in the west of the Amuria microcontinent. This does not contradict our interpretation, since a continental contact appears possible in the west of Amuria in the reconstruction of Fig. 13. A large, probably oceanic, bay, however, still existed in the Late Permian, the width of which could reach 3500–5300 km between Alentuy and Belektuy formation localities, which have been close to the shore of the Siberia and Amuria blocks, respectively.

In the Middle–Late Jurassic, the Shadaron pole is problematic, and so we prefer to use the reliable INM pole of Zhao *et al.* (1990). Our reconstruction (Fig. 13a) suggests that the ocean (1800 km minimum width, which is the difference between Badin and INM locality poles) still exists even at the longitude of the Shadaron formation, as the closest Late Jurassic pole of INM is consistent with the NCB pole. Geological evidence, however, somewhat contradicts this interpretation. In effect, no marine sediments of this age are found in the Trans-Baikal area. We note, however, that they do exist in the eastern part of this system, in the Amur Province (Krasniy 1966). After Zonenshain *et al.* (1990), the Trans-Baikal granitoids are Triassic–Early Jurassic in age, and Zonenshain & Kuzmin (1997) suggest that the Late Jurassic granitoid and basaltic magmatism exposed there must be considered as intraplate. These authors therefore suggest a closure of the ocean no later than the middle Jurassic. The zones of greenschist metamorphism, granite-gneissic domes, and granitoid batholiths were interpreted as indicators of continental collision. Moreover, three groups of geological complexes indicating former convergence have been distinguished (Zonenshain *et al.* 1990; Zonenshain & Kuzmin 1997): (1) terrestrial calc-alkaline volcanics on the rim of the belt; (2) tholeitic and calc-alkaline magmatic series associated with clastic and turbidite sequences within the belt, including gabbro-tonalitic intrusions of the Pikan and Bereya complexes (Fig. 1); and (3) chaotic complexes. These complexes could be related to a subduction zone in the Mongol–Okhotsk basin in the Early Mesozoic (due to geological and absolute dating data). Ophiolites are present along the suture in a few zones (Onon, Udurgin, Ust-Borzja, Urtuy, Djorol). These data indicate that remnants of the oceanic floor of two marine basins (Late Precambrian and Middle Palaeozoic) are present within the suture. For example, Misnik & Shevchuk (1980) showed that in the Djorol zone dynamic and thermal metamorphism of greenschists and gabbro-amphibolites with serpeninite slabs was synchronous with motions and deformations along the Mongol–Okhotsk suture. These authors showed a Mesozoic age of metamorphism. Some tectonic events occurred later than the Early Jurassic, however, because the Djorol ophiolites are thrust over Lower Mesozoic rocks, while serpentinite melanges contain fragments of Jurassic granites. On the other hand, our data and the INM data of Zhao *et al.* (1990) indicate a palaeolatitude gap between the Amuria and the south of Siberia.

There are several possible explanations for this discrepancy, among which is some amount of intracontinental shortening following an early collision. This, however, might be insufficient to explain the 2650 ± 840 km of observed palaeolatitude difference. Marine sediments are well known in the eastern part of the suture (Zonenshain *et al.* 1990), and final closure of the Mongol–Okhotsk Ocean took place after the Late Jurassic. This interpretation is corroborated by the comparison of the palaeoposition of Amuria from INM (Zhao *et al.* 1990) and Badin data. If we take the average palaeolatitudes at their face values, the difference between the INM block (37.6° for Manzhouli area; Zhao *et al.* 1990) and Badin formation (62.1°)

could denote this northward motion of the Amuria block with respect to Siberia ($\Delta_{palaeolat} = 23.9^\circ \pm 7.6^\circ$, when the present-day latitude difference $\Delta_{lat} = 2.3^\circ$). If we suppose a closing time of 20 Myr, during the Late Jurassic and the beginning of the Early Cretaceous (i.e. between 160 and 140 Ma), with a mean estimate of the initial width of 2650 km, the Mongol–Okhotsk Ocean could have closed at an average speed of 13.3 cm yr^{-1}. This value, albeit high, is not inconceivable. If closure of the ocean lasted 40 Ma, this speed might be two times less.

Finally, a general scheme that emerges from this analysis is that the Mongol–Okhotsk Ocean indeed existed in the Late Permian, with a width as large as 4700 km, which was reduced slightly during the Triassic, where we have no data, and closed relatively quickly at the end of the Jurassic–beginning of the Early Cretaceous. Accounting for Early Permian collision evidence in the west of the system, the large Late Jurassic palaeolatitude differences in the Trans-Baikal area, and the post-Early Cretaceous closure suspected in the east by Halim *et al*. (1998a), this ocean probably closed in a 'scissor-like' way (Zonenshain *et al*. 1990; Zhao *et al*. 1990) between the Early Permian and Early Cretaceous, with a drastic acceleration of this closure at the end of Jurassic.

ACKNOWLEDGMENTS

The authors express their deep gratitude for assistance in conducting the work and for valuable advice to A. N. Zhitkov, K. M. Konstantinov, and V. M. Asoskov. This study was initiated after discussion with and with the help of A. Ya. Kravchinsky and L. P. Zonenshain. Special thanks for geological information and field trip help go to palaeontologists V. M. Skoblo, N. A. Lyamina, N. A. Truzheva, and geologists S. I. Drill, and M. Kazimirovsky. VAK thanks V. Courtillot, J. Besse, and J.-P. Valet for invitation in IPGP, and J. Mivielle for help during his stay in France. R. Enkin supplied us with his free computer programs. We thank V. Courtillot and S. Gilder for their important and useful comments during the preparation of this manuscript. R. Enkin and another anonymous reviewer provided useful comments and corrections. VAK thanks Eddi and Irina Warré, and Bernard and Larissa Robin for their kind help in organizing life in France. The research was funded by the Geological Committee of Russia, Siberian Branch of the Russian Academy of Sciences, the Institut de Physique du Globe de Paris, and the 'Chita-geologija' state geological enterprise. VAK and MIK were partly supported by the International Science Foundation of G. Soros (Project NNAOO). This is contribution 1773 of the Institut de Physique du Globe de Paris.

REFERENCES

Besse, J. & Courtillot, V., 1991. Revised and synthetic apparent polar wander paths of African, Eurasian, North-American and Indian true polar wander since 200 Ma, *J. geophys. Res.,* **96,** 4029–4050.

Burov, B.V., Nurgaliev, D.K. & Yasonov, P.G., 1986. *Paleomagnetic Analysis,* Publishing House of Kazan University, Kazan (in Russian).

Dmitriev, G.A. & Rozhdestvensky, A.K., 1968. Bone-bearing facies of lake–river sediments of Upper Mesozoic of Buriat Republic, in *Mesozoic and Cenozoic Lakes of Siberia,* pp. 39–49, eds Kozlovsky, V.I., Nauka, Moscow (in Russian).

Enkin, R.J., 1990. Formation et deformation de l'Asie depuis la fin de l'ere primaire: les apports de l'etude paleomagnetique des formations secondaires de Chine du Sud, *PhD thesis,* University of Paris 7, Paris.

Enkin, R.J., 1996. *A Computer Program Package for Analysis and Presentation of Paleomagnetic Data,* Pacific Geoscience Center, Geological Survey of Canada, http://www.pgc.nrcan.gc.ca/tectonic/enkin.htm.

Enkin, R.J., Yang, Z., Chen, Y. & Courtillot, V., 1992. Paleomagnetic constraints on the geodynamic history of the major blocks of China from the Permian to the Present, *J. geophys. Res.,* **97,** 13 953–13 989.

Fisher, R., 1953. Dispersion on a sphere, *Proc. R. Soc. Lond., A,* **217,** 295–305.

Gilder, S. & Courtillot, V., 1997. Timing of the North–South China collision from new middle to late Mesozoic paleomagnetic data from the North China Block, *J. geophys. Res.,* **102,** 17 713–17 727.

Gilder, S., Zhao, X., Coe, R., Meng, Z., Courtillot, V. & Besse, J., 1996. Paleomagnetism and tectonics of the southern Tarim basin, northwestern China, *J. geophys. Res.,* **101,** 22 015–22 031.

Halim, N., Kravchinsky, V., Gilder, S., Cogné, J.-P., Alexutin, M., Sorokin, A., Courtillot, V. & Chen, Y., 1998a. A palaeomagnetic study from the Mongol-Okhotsk region: rotated Early Cretaceous volcanics and remagnetized Mesozoic sediments, *Earth planet. Sci. Lett.,* **159,** 133–145.

Halim, N., Cogné, J.-P., Chen, Y., Atasiei, R., Besse, J., Courtillot, V., Gilder, S., Marcoux, J. & Zhao, R.L., 1998b. New Cretaceous and Early Tertiary paleomagnetic results from Xining-Lanzhou basin, Kunlun and Qiangtang blocks, China: Implications on the geodynamic evolution of Asia, *J. geophys. Res.,* **103** (B9), 21 025– 21 045.

Halls, H.C., 1976. A least-squares method to find a remanence direction from converging remagnetization circles, *Geophys. J. R. astr. Soc.,* **45,** 297–304.

Jelinek, V., 1966. A high sensitive spinner magnetometer, *Stud. Geophys. Geod.,* **10,** 58–78.

Jelinek, V., 1973. Precision A.C. bridge set for measuring magnetic susceptibility and its anisotropy, *Stud. Geophys. Geod.,* **17,** 36–48.

Kirschvink, J.L., 1980. The least-squares line and plane and the analysis of paleomagnetic data, *Geophys. J. R. astr. Soc.,* **62,** 699–718.

Kozubova, L.A. & Radtchenko, G.P., 1961. *New Data on Age Determination of Volcanogenic Rocks of Dzida-Khilok Serie in Wastern Trans-Baikal Region,* Nedra, Leningrad (in Russian).

Krasniy, L.I. (ed.), 1966. *Geology of the USSR, Khabarovsk and Amur Provinces,* Nedra, Moscow (in Russian).

Kravchinsky, V.A., 1990. Paleomagnetism of rocks of Mongol-Okhotsk Geosuture, in *Publication of the IGCP project Nos 224 and 283,* pp. 146–149, eds Dobrefsov, N.L., Institute of Geology and Geophysics, Siberian Branch of the Academy of Sciences of the USSR, Novosibirsk.

Kravchinsky, V.A., 1995. Paleomagnetic study in Mongol-Okhotsk folded belt, *PhD thesis,* Irkutsk State Technical University, Irkutsk (in Russian).

Kuzmin, M.I., 1985. *Geochemistry of Magmatic Rocks of Phanerozoic Mobil Fold Belts,* Nauka, Novosibirsk (in Russian).

Kuzmin, M.I. & Fillipova, I.B., 1979. The history of the Mongol-Okhotsk belt in the Middle–Late Paleozoic and Mesozoic, in *Lithospheric Plate Structure,* pp. 189–226, ed. Zonenshain, L.P., Institute of Oceanology, USSR Acad. Sci., Moscow, (in Russian).

Kuzmin, M.I. & Kravchinsky, V.A., 1996. First paleomagnetic data for Mongol-Okhotsk fold belt, *Russian J. Geol Geophys.,* **37,** 54–62. (in Russian).

Li, Y.P., Zhang, Z.K., McWilliams, M., Sharps, R., Zhai, Y.J., Li, Y.A., Li, Q. & Cox, A., 1988. Mesozoic paleomagnetic results of the Tarim craton: Tertiary relative motion between China and Siberia, *Geophys. Res. Lett.,* **15,** 217–220.

Likhanov, V.D. (ed.), 1991. Geological composition and mineral resources of Ortinka and North Gareka Rivers basins, *Report of Verkhne-Garikan geological expedition of the State Geological Enterprise, 'Chitageologija'* (in Russian).

Lyamina, N.A., Skoblo, V.M., Luzina, I.V. & Rudnev, A.F., 1998. New data for stratigraphy of Irkutsk basin Jurassic age (Abstract), in *Problems of Geology and Producing of Mineral Resources in East Siberia,* pp. 52–53, Irkutsk State University, Irkutsk (in Russian).

McElhinny, M.W., 1964. Statistical significance of the fold test in paleomagnetism, *Geophys. J. R. astr. Soc.,* **8,** 338–340.

McElhinny, M.W. & Lock, J., 1996. IAGA paleomagnetic databases with access, *Surv. Geophys.,* **17,** 575–591.

McFadden, P.L. & Lowes, F.J., 1981. The discrimination of mean directions drawn from Fisher distributions, *Geophys. J. R. astr. Soc.,* **67,** 19–33.

McFadden, P.L. & McElhinny, M.W., 1988. The combined analysis of remagnetization and direct observation in paleomagnetism, *Earth planet. Sci. Lett.,* **87,** 161–172.

McFadden, P.L. & McElhinny, M.W., 1990. Classification of the reversal test in paleomagnetism, *Geophys. J. Int.,* **103,** 725–729.

Misnik, Yu.F. & Shevchuk, V.V., 1980. The East-Trans-Baikal ancient block and its role in formation of the regional structure, *Geotectonika,* **5,** 25–37 (in Russian).

Nei, S., 1991. Paleoclimatic and paleomagnetic constraints on the Paleozoic reconstructions of South China, North China and Tatim, *Tectonophysics,* **196,** 279–308.

Neustroeva, I.Yu., 1988. History of non-sea Paleozoic and Mesozoic ostracoda developing after mobilism conseption, in *Formation and Evolution of Continental Biotas, Proc. XXXI Session Paleontological Society,* pp. 60–69, Nauka, Leningrad (in Russian).

Parfenov, L.M., 1984. *Continental Margins and Island Arcs of Mesozoids of North-Western Asia,* Nauka, Novosibirsk (in Russian).

Pavlov, V.E., 1993. Paleomagnetic directions and paleomagnetic pole positions: Data for the former USSR, Issue 8, *VNIGRI Institute, St. Petersburg (unpublished Catalogue)*

Pisarevsky, S.A., 1982. Paleomagnetic directions and paleomagnetic pole positions: Data for the USSR, Issue 5, *Soviet Geophysical Committee, World Data Center-B (Moscow) Catalogue.*

Pospelova, G.A., 1971. Paleomagnetic directions and pole positions: Data for the USSR, Issue 1, *Soviet Geophysical Committee: World Data Center-B (Moscow), Catalogue.*

Pruner, P., 1992. Paleomagnetism and paleogeography of Mongolia in the Cretaceous, Permian and Carboniferous—final report, *Phys. Earth planet. Inter.,* **70,** 169–177.

Shubkin, S.P., Beljakov, E.A. & Boljakov, I.P., 1992. Geological composition and mineral resources of Unda and Kurenga rivers basins, *Report of Siviinskaya Geological Expedition About Results of Geological Study During 1987–1991 Years, Scale 1: 50000,* Chita region State geological enterprise 'Chitageologija'.

Sinitsa, S.M. & Starukhina, L.P., 1986. New data and problems of stratigraphy and paleontology of Upper Mesozoic of Trans-Baikal region, in *New Data on Trans-Baikal Geology,* pp. 46–51, Geological State Company, Chita.

Skoblo, V.M. & Lyamina, N.A., 1982. *Methodological Guidelines on Usage of Paleontological Horizons and Lithological Coefficients for Dismembering and Correlation of Continental Deposits, Exemplified by Western Trans-Baikalia,* VSNIIGGIMS, Ministry of Geology of the USSR, Irkutsk (in Russian).

Skoblo, V.M. & Lyamina, N.A., 1985. Irkutsk basin, Western and Eastern Trans-Baikalia, in *Jurassic Continental Biosenoses of South Siberia and Surrounded Territories,* pp. 41–56, Nauka, Moscow (in Russian).

Skoblo, V.M., Rudnev, A.F., Lyamina, N.A. & Vittenberg, T.B., 1991. Biostratigraphic and litho-facial investigations of the basic outcrops of Mesozoic for legend of Irkutsk series of maps of scale 1:50,000, *Information Report on a Theme 1423419126 for 1989–1990 Years,* East–Siberian Research Institute of Geology, Geophysics and Mineral Resources, Irkutsk (in Russian).

Skoblo, V.M., Fillipov, A.G. & Lyamina, N.A., 1994. Continental Mesozoic and Cenozoic of Trans-Baikal and Pri-Baikal regions, in *Geology, Mineral Resources and Geoecology of South Part of Eastern Siberia,* ed. Mitrofanov, G.L., pp. 21–27, Siberian Branch of Russian Academy of Science and East Siberian Research Institute of Geology, Geophysics and Mineral Resources, Irkutsk.

Sorokin, A.A., 1992. Geochemistry and geodynamic position of magmatic rocks of the central segment of the Mongol-Okhotsk fold belt, *PhD thesis,* Institute of Geochemistry, Siberian Branch of the Russian Academy of Science, Irkutsk (in Russian).

Van der Voo, x, 1966. *Stratigraphy of the USSR. Permian System,* Nedra, Moscow (in Russian).

Van der Voo, R., 1993. *Paleomagnetism of the Atlantic, Tethis, and Iapetus Oceans,* Cambridge University Press, Cambridge.

Vinarsky, Ya.S., Zhitkov, A.N. & Kravchinsky, Ya.A., 1987. Automated system OPAL for processing paleomagnetic data, Algorithms and programs, Issue 10/99/VIAMS, VIAMS, Moscow, (in Russian).

Watson, G.S. & Enkin, R.J., 1993. The fold test in paleomagnetism as a parameter estimation problem, *Geophys. Res. Lett.,* **20,** 2135–2137.

Xu, X., Harbert, W., Drill, S. & Kravchinsky, V., 1997. New paleomagnetic data from the Mongol-Okhotsk collision zone, Chita region, south-central Russia: implications for Paleozoic paleogeography of the Mongol-Okhotsk ocean, *Tectonophysics,* **269,** 113–129.

Yang, Z. & Besse, J., 2001. New Mesozoic apparent polar wandering path for South China: tectonic consequences, *J. geophys. Res.,* **106,** 8493–8520.

Yang, Z., Courtillot, V., Besse, J., Ma, X., Xing, L., Xu, S. & Zhang, J., 1992. Jurassic paleomagnetic constrains on the collision of the North and South China blocks, *Geophys. Res. Lett.,* **6,** 577–580.

Yanshin, A.L., 1981. *Geological Map of East Siberia, South and Northern Part of Mongolia,* VSEGEI, Leningrad.

Zhao, X., Coe, R.S., Zhou, Y.X., Wu, H.R. & Wang, J., 1990. New palaeomagnetic results from northern China: collision and suturing with Siberia and Kazakhstan, *Tectonophysics,* **181,** 43–81.

Zhao, X., Coe, R.S., Gilder, S.A. & Frost, G.M., 1996. Paleomagnetic constraints on the palaeogeography of China: implications for Gondwanaland, *Aus. J. Earth Sci.,* **xx**, 643–672.

Zijderveld, J.D.A., 1967. A.C. demagnetization of rocks, analysis of results, in *Methods in Paleomagnetism,* pp. 254–286, eds Collinson, D.W., Creer, K.M. & Runcorn, S.K., Elsevier, Amsterdam.

Zonenshain, L.P. & Kuzmin, M.I., 1997. *Paleogeodynamics,* Am. geophys. Un., Washington.

Zonenshain, L.P., Kuzmin, M.I. & Moralev, V.M., 1976. *Global Tectonics, Magmatism and Metallogeny,* Nedra, Moscow (in Russian).

Zonenshain, L.P., Kuzmin, M.I. & Natapov, L.M., 1990. *Tectonics of Lithosphere Plates of the Territory of the USSR,* Nedra, Moscow (in Russian).